

1 Nitrogen restricts future treeline advance in the sub-arctic

2 Adrian Gustafson^{1,2}, Paul A. Miller^{1,2}, Robert G. Björk^{4,5}, Stefan Olin¹, Benjamin Smith^{1,3}

3 ¹Department of Physical Geography and Ecosystem Science, Lund University, Sölvegatan 12, 223 62 Lund, Sweden

4 ²Center for Environmental and Climate Science, Lund University, Sölvegatan 37, 223 62, Lund, Sweden

5 ³Hawkesbury Institute for the Environment, Western Sydney University, Penrith, NSW 2751, Australia

6 ⁴Department of Earth Sciences, University of Gothenburg, P.O. Box 460, SE-40530 Gothenburg, Sweden

7 ⁵Gothenburg Global Biodiversity Centre, P.O. Box 461, SE-405 30 Gothenburg, Sweden

8 *Correspondence to:* adrian.gustafson@nateko.lu.se

9 **Abstract.** Arctic environmental change has induced shifts in high latitude plant community composition and stature
10 with implications for Arctic carbon cycling and energy exchange. Two major components of high latitude ecosystems
11 undergoing change is the advancement of trees into treeless tundra and the increased abundance and size of shrubs.
12 How future changes in key climatic and environmental drivers will affect distributions of major ecosystem types is an
13 active area of research. Dynamic Vegetation Models (DVMs) offer a way to investigate multiple and interacting drivers
14 of vegetation distribution and ecosystem function. We employed the LPJ-GUESS DVM over a subarctic landscape in
15 northern Sweden, Torneträsk. Using a highly resolved climate dataset we downscaled CMIP5 climate data from three
16 Global Climate Models and two 21st century future scenarios (RCP2.6 and RCP8.5) to investigate future impacts of
17 climate change on these ecosystems. We also performed three model experiments where we factorially varied drivers
18 (climate, nitrogen deposition and [CO₂]) to disentangle the effects of each on ecosystem properties and functions. We
19 found that treelines could advance by between 45 and 195 elevational meters in the landscape until the year 2100, de-
20 pending on the scenario. Temperature was a strong, but not the only, driver of vegetation change. Nitrogen availability
21 was identified as an important modulator of treeline advance. While increased CO₂ fertilisation drove productivity in-
22 creases it did not result in any range shifts of trees. Treeline advance was realistically simulated without any tempera-
23 ture dependence on growth, but biomass was overestimated. As nitrogen was identified as an important modulator of
24 treeline advance, we support the idea that accurately representing plant-soil interactions in models will be key to future
25 predictions of Arctic vegetation change.

26 **Keywords:** Ecosystem model, forest-tundra ecotone, treeline, sub-Arctic, climate change impacts, ecosystem stability,
27 LPJ-GUESS, biogeophysical feedbacks.

28 1. Introduction

29 In recent decades, the Arctic has been observed to become greener (Epstein et al., 2012; Bhatt et al., 2010). Causes
30 include an increased growth and abundance of shrubs (Myers-Smith et al., 2011; Elmendorf et al., 2012; Forbes et al.,
31 2010), increased vegetation stature associated with a longer growing season, and poleward advance of the Arctic
32 treeline (Bjorkman et al., 2018). Shrubs protruding through the snow and treeline advance will alter surface albedo and
33 energy exchange with potential feedback to the climate system (Chapin et al., 2005; Sturm, 2005; Serreze and Barry,
34 2011; Zhang et al., 2013; Zhang et al., 2018). Warming and associated changes in high latitude ecosystems have impli-

35 cations for carbon cycling through increased plant productivity and species shifts (Chapin et al., 2005; Zhang et al.,
36 2014), but also increased soil organic matter (SOM) decomposition with subsequent loss of carbon to the atmosphere.
37 Studies of the Arctic carbon balance have shown that the Arctic has been a weak sink in the past (Mcguire et al., 2009;
38 Mcguire et al., 2012; Bruhwiler et al., 2021; Virkkala et al., 2021), although uncertainty is substantial, and it is difficult
39 to determine accurately the strength of this sink. How climate and environmental changes will affect the relative bal-
40 ance between the carbon uptake, i.e. photosynthesis, and release processes, i.e., autotrophic and heterotrophic respira-
41 tion, will determine whether the Arctic will be a source or a sink of carbon in the future.

42 Forest-tundra ecotones constitute one of the largest transition zones where abrupt changes in ecosystem functioning
43 occur (Hofgaard et al., 2012). While no generally accepted theory of what drives treeline advance has been put forward,
44 several alternative explanations exist. Firstly, direct effects of rising temperatures have been thoroughly discussed (e.g.,
45 Rees et al., 2020; Hofgaard et al., 2019; Körner, 2015; Chapin, 1983). On the global scale, treelines have been found to
46 correlate well with a 6-7°C mean growing season ground temperature (Körner and Paulsen, 2004) and could thus be
47 expected to shift with rising temperatures. A global study of alpine treeline advance in response to warming since 1900
48 shows that 52% of treelines had advanced while the other half was stationary (47%), with only occasional instances of
49 retreat (1%) (Harsch et al., 2009). Similar patterns have been observed on the circumarctic scale, although latitudinal
50 treelines might be expected to shift more slowly than elevational treelines due to dispersal constraints (Rees et al.,
51 2020). As trees close to the treeline often show ample storage of non-structural carbohydrates (Hoch and Körner, 2012)
52 it has been suggested that a minimum temperature requirement for wood formation, rather than productivity, constrains
53 treeline position (Körner, 2003, 2015; Körner et al., 2016).

54 Secondly, it has been hypothesised that indirect effects of warming might be equally or more important than direct
55 effects (Sullivan et al., 2015; Chapin, 1983). For example, rising temperatures and subsequently soil temperatures might
56 induce increased nitrogen mineralisation and plant nitrogen uptake (Chapin, 1983). Increased nitrogen uptake could in
57 turn enhance plant productivity and growth (Dusenge et al., 2019). Increased nitrogen uptake as a consequence of in-
58 creased soil temperatures or nitrogen fertilisation have been shown to increase seedling winter survival among moun-
59 tain birch (*Betula pubescens ssp. tortuosa*) seedlings (Weih and Karlsson, 1999; Karlsson and Weih, 1996).

60 Thirdly, experiments of elevated CO₂ often show increased plant productivity and biomass increase, especially in trees
61 (Ainsworth and Long, 2005). Terrestrial biosphere models generally agree with this pattern (Hickler et al., 2008; Smith
62 et al., 2014; Piao et al., 2013). Although difficult to measure in field experiments, treeline position seems unresponsive
63 to increased [CO₂] alone (Holtmeier and Broll, 2007). Whether treelines are responsive to increased productivity
64 through CO₂ fertilisation might yield insights into whether treelines are limited by their productivity, i.e., photosynthe-
65 sis, or ability to utilise assimilated carbon, i.e., wood formation. However, to what extent increased [CO₂] drives long-
66 term tree and shrub encroachment and growth remains poorly studied.

67 For treeline migration to occur, it is not only the growth and increased stature of established trees that is important, but
68 also the recruitment and survival of new individuals beyond the existing treeline (Holtmeier and Broll, 2007). Seedlings
69 of treeline species are sometimes observed above the treeline, especially in sheltered microhabitats (Hofgaard et al.,
70 2009; Sundqvist et al., 2008). However, these individuals often display a stunted growth and can be up to a few decades

71 old, although age declines with elevation (Hofgaard et al., 2009). The suitability of the tundra environment for trees to
72 establish and grow taller will thus be an important factor for the rate of treeline advance (Cairns and Moen, 2004). In-
73 terspecific competition and herbivory are known to be important modulators of range shifts of trees (Cairns and Moen,
74 2004; Van Bogaert et al., 2011; Grau et al., 2012). For instance, the presence of shrubs has been shown to limit tree
75 seedling growth (Weih and Karlsson, 1999; Grau et al., 2012), likely as a consequence of competition with tree seed-
76 lings for nitrogen. Comparisons of models incorporating only bioclimatic limits to species distributions and a more
77 ecologically complex model have also revealed interspecific plant competition to be important for range shifts of trees
78 (Scherrer et al., 2020; Epstein et al., 2007). Thus, as a fourth factor, shrub-tree interactions are likely to be important
79 when predicting forest range shifts under future climates. Rising temperatures have been suggested as the dominant
80 driver of increased shrub growth, especially where soil moisture is not limiting (Myers-Smith et al., 2015; Myers-Smith
81 et al., 2018). Furthermore, a changed precipitation regime, especially increased winter snowfall, might promote estab-
82 lishment of trees and shrubs through the insulating effects of snow cover with subsequent increases in seedling winter
83 survival (Hallinger et al., 2010).

84 A narrow focus on a single, e.g., summer temperature, or a few driving variables may lead to overestimations of treeline
85 advance in future projections (Hofgaard et al., 2019). Dynamic vegetation models (DVMs) offer a way to investigate
86 the influence of multiple and interacting drivers on vegetation and ecosystem processes. Model predictions may be
87 compared with observations of local treelines and ecotones to validate assumptions embedded in the models, and to
88 interpret causality in observed dynamics and patterns. DVMs also offer a way to extrapolate observable local phenome-
89 na to broader scales, such as that of circumarctic shifts in the forest-tundra ecotone and the responsible drivers. Here,
90 we examine a subarctic forest-tundra ecotone that has undergone spatial shifts over recent decades (Callaghan et al.,
91 2013), previously attributed to climate warming. Adopting a DVM incorporating a detailed description of vegetation
92 composition and stature and nitrogen cycle dynamics, we apply the model at high spatial resolution to compare ob-
93 served and predicted recent treeline dynamics, and project future vegetation change with implications for carbon bal-
94 ance and biogeophysical feedbacks. In addition, we conduct three model experiments to separate and interpret the im-
95 pact of driving factors (climate, nitrogen deposition, [CO₂]) on vegetation in a forest-tundra ecotone in Sweden's sub-
96 arctic north.

97 **2. Materials and Methods**

98 **2.1 Abisko**

99 Abisko Scientific Research station (ANS; 68°21' N, 18°49' E) has a long record of ecological and climate research. The
100 climate record date back to 1913 and is still ongoing. The research station is situated in a rain shadow and is thus rela-
101 tively dry despite its proximity to the ocean (Callaghan et al., 2013). The research station is situated in the valley, close
102 to the lake Torneträsk. The forests in the lower parts of the valley consist mostly of mountain birch *Betula pubescens*
103 *ssp. czerepanovii* which is also dominant at the treeline. Treeline elevation in the Abisko valley range between 600-800
104 m above sea level (a.s.l.) (Callaghan et al., 2013). Other tree types in lower parts of the valley are *Sorbus aucuparia*,
105 and *Populus tremula*, along with small populations of *Pinus sylvestris* which are assumed to be refugia species from

106 warmer periods during the Holocene (Berglund et al., 1996). Soils are glaciofluvial till and sediments. A full summary
107 of previous studies and the environment around lake Torneträsk can be found in Callaghan et al. (2013).
108 Our study domain covers an area of approximately 85 km² and extends from Mount Njulla in the west to the mountain
109 Nissoncorru in the East (See Fig. 2). In the northern part of our study domain is the lake Torneträsk. The mean annual
110 temperature was -0.5 ± 0.9 °C for the 30-year period 1971-2000 (Fig. 1; Table 2) with January as the coldest month ($-$
111 10.2 ± 3.5 °C) and July as the warmest month (11.3 ± 1.4 °C). Mean annual precipitation was 323 ± 66 mm for the
112 same reference period. This reference period was chosen as it is the last one in the dataset by Yang et al. (2011).

113 **2.2 Ecosystem model**

114 We used the LPJ-GUESS DVM as the main tool for our study (Smith et al., 2001; Smith et al., 2014; Miller and Smith,
115 2012). LPJ-GUESS is one of the most ecologically detailed models of its class, suitable for regional and global-scale
116 studies of climate impacts on vegetation, employing an individual- and patch-based representation of vegetation com-
117 position and structure. It simulates the dynamics of plant populations and ecosystem carbon, nitrogen, and water ex-
118 changes in response to external climate forcing. Biogeophysical processes (e.g. soil hydrology and evapotranspiration)
119 and physiological processes (e.g. photosynthesis, respiration, carbon allocation) are both closely linked and represented
120 mechanistically. The model assumes the presence of seeds in grid cells, meaning that simulated PFTs can establish once
121 the climate is favourable, as defined by each PFT's predefined bioclimatic limits. The competition between neighbour-
122 ing plant individuals for light, water and nutrients, affecting individual establishment, growth, and mortality, is mod-
123 elled explicitly. Individuals of the same age co-occurring in a local neighbourhood or patch and belonging to the same
124 plant functional type (PFT; see below) are assumed identical to each other. Decomposition of plant litter and cycling of
125 soil nutrients are represented by a CENTURY-based soil biogeochemistry module, applied at patch scale (Smith et al.,
126 2014). Biological N fixation is represented by an empirical relationship between annual evapotranspiration and nitrogen
127 fixation (Cleveland et al., 1999) and occurs differently within each patch. Additional inputs of nitrogen to the system
128 occur through nitrogen deposition or fertilisation. Nitrogen is lost from the system through leaching, gaseous emissions
129 from soils and wildfires. For a full description of the nitrogen cycle in LPJ-GUESS, see Smith et al. (2014).

130 For this study we employed LPJ-GUESS version 4.0 (Smith et al. 2014), enhanced with Arctic-specific features (Miller
131 and Smith, 2012; Wania et al., 2009). The combined model incorporates an updated set of arctic PFTs (described be-
132 low), improved soil physics and a multi-layered dynamic snow scheme, allowing for simulation of permafrost and fro-
133 zen ground.

134 Vegetation in the model is represented by cohorts of individuals interacting in local communities or patches and belong-
135 ing to a number of PFTs that are distinguished by growth form (tree, shrub, herbaceous), life history strategies (shade
136 tolerant or intolerant), and phenology class (evergreen/summergreen). Herbaceous PFTs are represented as a dynamic,
137 aggregate cover of ground layer vegetation in each patch. In this study 11 PFTs were implemented (See Table S2.1 in
138 supplementary material for a description of included PFTs; see Table S2.2 in supplementary material for parameter
139 values associated with each PFT). Out of these, three were tree PFTs, boreal needle-leaved evergreen trees (BNE),
140 boreal shade-intolerant evergreen tree (BINE) and boreal shade-intolerant broad-leaved summergreen tree (IBS). Corre-
141 sponding tree species present in the Torneträsk region include *Picea abies* (BNE), *Pinus sylvestris* (BINE), *Betula pu-*

142 *bescens ssp. czerepanovii*, *Populus tremula* and *Sorbus aucuparia* (IBS). Following Wolf et al. (2008), shrub PFTs with
143 different stature were implemented as follows: tall summergreen and evergreen shrubs, corresponding to *Salix spp.*
144 (HSS) and *Juniperus communis* (HSE) and low summergreen and evergreen shrubs. The two latter corresponding to
145 species such as *Betula nana* (LSS) and *Empetrum nigrum* (LSE). We also include two prostrate shrubs and two herba-
146 ceous PFTs.

147 Gridcell vegetation and biogeophysical properties are calculated by averaging over a number of replicate patches, each
148 subject to the same climate forcing. No assumptions are made about how the patches are distributed within a gridcell,
149 they are a statistical sample of equally possible disturbance/demographic histories across the landscape of a gridcell.
150 Within each patch, establishment, growth and mortality of individual tree or shrub cohorts are modelled annually
151 (Smith et al., 2001; Smith et al., 2014). Establishment and mortality have both an abiotic (bioclimatic) and biotic (com-
152 petition-mediated) component. Vegetation dynamics, i.e. changes in the distribution and abundance of different PFTs in
153 grid cells over time, are an emergent outcome of the competition for resources between PFTs within an overall climate
154 envelope determined by bioclimatic limits for establishment and survival. The bioclimatic envelope is a hard limit to
155 vegetation distribution, intended to represent the physiological niche of a PFT. Furthermore, the climate envelope is a
156 proxy for physiological processes such as meristem activity that may set species ranges, but also for climatic stressors
157 such as tissue freezing. Disturbance is accounted for by the occasional removal of all vegetation within a patch with an
158 annual probability of one per 300 years, representing random events such as storms, avalanches, insect outbreaks, and
159 wind-throw. The study used three replicate patches within each 50x50m gridcell.

160 For summergreen PFTs we slightly modified the assumption of a fixed growing degree day (GDD) requirement for
161 establishment, using thawing degree days (TDD; degree days with a 0 °C basis; see Table S2.2) instead.

162 **2.3 Forcing data**

163 **2.3.1 Historic period**

164 A highly resolved (50x50m) temperature and radiation dataset using field measurements and a digital elevation model
165 (DEM) by Yang et al. (2011) provided climate input to the model simulations for the historic period (1913-2000). The
166 field measurements were conducted in form of transects that captured mesoscale climatic variations, i.e., lapse rates. In
167 addition, the transects were placed to capture microclimatic effects of the nearby lake Torneträsk and variations in radi-
168 ation stemming from mountainside aspect. The temperature in the lower parts of the Abisko valley in the resulting da-
169 taset was influenced by the lake with milder winters and less yearly variability. At higher elevation, the temperature was
170 more variable over the year and the local scale variations were more dependent on the different solar angles between
171 seasons and mountainside aspect (Yang et al., 2011; Yang et al., 2012)(see Fig. S1.1; supplementary materials). For a
172 full description of how this dataset was constructed we refer to Yang et al. (2011) and Yang et al. (2012).

173 Monthly precipitation input was obtained from the Abisko Scientific Research Station weather records. Precipitation
174 was randomly distributed over each month using probabilities from the CRUNCEP v.7 dataset (Wei et al., 2014). We
175 assumed that local differences in precipitation can be neglected for our study domain and thus the raw station data was
176 used as input to LPJ-GUESS for the historic period. Nitrogen deposition data for the historic and future simulations

177 were extracted from gridcell including Abisko in the dataset produced by Lamarque et al. (2013). Nitrogen deposition
178 was assumed to be distributed equally over the study domain.

179 Data of soil texture was extracted from the WISE soil dataset (Batjes, 2005) for the Abisko area and assumed to be
180 uniform across the study domain. Callaghan et al (2013) reports that the soils around the Torneträsk areas are mainly
181 glaciofluvial till and sediments. Clay and silt fractions vary between 20-50% in the area (Josefsson, 1990) with higher
182 fractions of clay and silt in the birch forest and a larger sand content in the heaths. In the absence of spatial information
183 on particle size distributions, the soil was prescribed as a sandy loam soil with approximately 43% sand and approxi-
184 mately equal fractions of silt and clay.

185 **2.3.2 Future simulations**

186 Future estimates of vegetation change were simulated for one low (RCP2.6) and one high (RCP8.5) emission scenario.
187 For each emission scenario, climate change projections from three global climate models (GCMs) that had contributed
188 to the CMIP5 GCM ensemble (Taylor et al., 2012) were used to investigate climate effects on vegetation dynamics. The
189 GCMs (MIROC-ESM-CHEM, HadGEM2-AO, GFDL-ESM2M) were selected to represent the largest spread, i.e.,
190 highest, lowest and near average, in modelled mean annual temperature for the reference period 2071-2100. Only mod-
191 els that had contributed with simulations for both RCP2.6 and RCP8.5 were used in the selection. Monthly climate data
192 needed as input to LPJ-GUESS (temperature, total precipitation, and shortwave radiation) was extracted for the gridcell
193 including ANS for each GCM.

194 The historic climate dataset by Yang et al (2011) was extended into the projection period (2001-2100) using the delta
195 change approach, as follows. For each gridcell monthly differences were calculated between the projection climate and
196 the dataset by Yang et al. (2011) for the last 30-year reference period in our historic dataset (1971-2000). For tempera-
197 ture, the difference was derived, while for precipitation and incoming shortwave radiation relative differences between
198 the two datasets were derived. The calculated monthly differences were then either added (temperature) to the GCM
199 outputs, or used to multiply (precipitation, radiation) the GCM outputs from 2001-2100, for each of the climate scenari-
200 os used. Forcing data of atmospheric [CO₂] for the two scenarios were collected from the CMIP5 project.

201 **2.4 Model experiments**

202 To investigate the possible drivers of future vegetation change we performed three model experiments. The model was
203 forced with changes to one category of input (driver) variables (climate, [CO₂], nitrogen deposition) at a time for a
204 projection period between the years 2001-2100. A full list of simulations can be found in Table S3 (supplementary
205 materials).

206 A control scenario with no climate trend (and with [CO₂] and nitrogen deposition held at their respective year 2000
207 values) was also created. We estimated the effect of the transient climate change, [CO₂] or nitrogen deposition scenarios
208 by subtracting model results for the last decade (2090-2100) in the no-trend scenario from those for the last decade
209 (2090-2100) of the respective transient scenario. To estimate how sensitive the model was to different factors, we per-

210 formed a Spearman rank correlation for each PFT in 50 m elevational bands over the forest-tundra ecotone. We chose
211 Spearman rank over Pearson since not all correlations were linear.

212 **2.4.1 Climate change**

213 To estimate the sensitivity to climate change the same scenarios as for the future simulations (section 2.3.2) were used
214 while [CO₂] and nitrogen deposition were held constant at their year 2000 value.

215 Climate anomalies without any trend were created by randomly sampling full years in the last decade (1990-2000) from
216 the climate station data. The climate dataset was then extended using this data. The resulting climate scenario had the
217 same inter-annual variability as the historic dataset and no trend for the years 2001-2100. This scenario was used to
218 investigate any lag-effects on vegetation change. This scenario also provided climate input for the nitrogen and [CO₂]
219 tests described below.

220 **2.4.2 CO₂**

221 For our projection simulations we used five different [CO₂] scenarios from the CMIP5 project. High (RCP8.5), medium
222 (RCP6.0; RCP4.5) and low (RCP2.6) emission scenarios were used.

223 **2.4.3 Nitrogen deposition**

224 Scenarios of nitrogen deposition were collected from the Lamarque et al. (2013) dataset. Since this dataset assumes a
225 decrease of nitrogen deposition after year 2000 we also added four scenarios where nitrogen deposition increased with
226 2, 5, 7.5 and 10 times the nitrogen deposition relative to the year 2000. These four scenarios were created to test the
227 isolated effect of nitrogen increase without any climate or [CO₂] change. The resulting additional loads of nitrogen in
228 these scenarios were 0.38, 0.97, 1.46 and 1.9 gN m⁻² yr⁻¹ respectively.

229 **2.5 Model evaluation**

230 We evaluated the model against a range of available observations in the Abisko area. Measurements of ecosystem
231 productivity from an eddy covariance (EC) tower were obtained for six non-consecutive years (Olsson et al., 2017).
232 Biomass and biomass change estimates were used to evaluate simulated biomass in the birch forest (Hedenås et al.,
233 2011). Surveys of historic vegetation change above the treeline were collected from Rundqvist et al. (2011). Leaf area
234 index (LAI) and evapotranspiration estimates were obtained from Ovhed and Holmgren (1996).

235 The two studies by Hedenås et al. (2011) and Rundqvist et al. (2011) documented evaluation measurements within our
236 projection period (year 2010). To compare biomass and vegetation change with these studies we extracted five year
237 multi-model averages around the year 2010 (2008-2012) from our projection simulations (section 2.3.2). These means
238 were used to calculate change in biomass and vegetation in our historic dataset.

239 To determine the local rates and heterogeneity of treeline migration several transects were selected within our study
240 domain (Fig. S1.2; supplementary material). These transects were chosen to represent a large spread in heterogeneity
241 with regard to slope and aspect in the landscape. A subsample of the selected transects were placed close to the tran-
242 sects used by Van Bogaert et al. (2011) and used to evaluate model performance. Results from the model evaluation are
243 summarised in Table 1 and Table S1.1.

244 **2.6 Determination of domains in the forest-tundra ecotone**

245 In our analysis we distinguished between forest, treeline and shrub-tundra, defined as follows. Any gridcell containing
246 30% fractional projective cover or more of trees was classified as forest. This limit has been used by other studies in the
247 area (e.g., Van Bogaert et al., 2011) to determine the birch forest boundary. The treeline was then determined by first
248 selecting gridcells classified as forest. Any gridcell with 4 or more neighbours fulfilling the 30% cover condition crite-
249 ria was classified as belonging to the forest. The perimeter of the forest was then determined through sorting out
250 gridcells with 4 or 5 neighbours classified as forest. Gridcells with fewer or more neighbors were regarded as tundra or
251 forest, respectively. Gridcells below the treeline were classified as forest in the analysis and gridcells above the treeline
252 were classified as tundra.

253 **2.7 Presentation of results**

254 We present seasonal values for soil and air temperature. These are averages of DJF, MAM, JJA, and SON, referred to
255 as winter, spring, summer and autumn below. For the RCPs average values are presented with the ranges of the differ-
256 ent scenarios within each RCP given in parenthesis. We report values of both gross primary production (GPP), which
257 we benchmark the model against, and net primary productivity (NPP) as this is of relevance for the carbon limitation
258 discussion.

259 **3. Results**

260 **3.1 Historic vegetation shifts**

261 The dominating PFT in the forest and at the treeline was IBS which constituted 90% of the total LAI (Fig. 2a-3a). The
262 only other tree PFT present in the forest was BINE, which comprised a minor fraction of total LAI. However, in the
263 lower (warmer) parts of the landscape BINE comprised up to 20% of total LAI in a few gridcells. Forest understory was
264 mixed but consisted mostly of tall and low evergreen shrubs and grasses. Shrub tundra vegetation above the treeline
265 was more mixed but LSE dominated with 51% of total LAI. Grasses comprised an additional 25% of total LAI and IBS
266 was present close to the treeline where it comprised up to 5% of LAI in some gridcells. NPP for IBS in the forest in-
267 creased from $96 \text{ gC m}^{-2} \text{ yr}^{-1}$ to $180 \text{ gC m}^{-2} \text{ yr}^{-1}$ over our historic period (1913-2000). Corresponding values at the
268 treeline did not increase but were stagnant at around $60 \text{ gC m}^{-2} \text{ yr}^{-1}$. Above the treeline, IBS showed very low NPP
269 values ($<15 \text{ gC m}^{-2} \text{ yr}^{-1}$), while NPP for the dominant shrub (LSE) doubled from $20 \text{ gC m}^{-2} \text{ yr}^{-1}$ to $40 \text{ gC m}^{-2} \text{ yr}^{-1}$.

270 Between the start and end of our historic (1913-2000) simulation the landscape scale treeline shifted upwards 67 eleva-
271 tional meters on average, corresponding to a rate of 0.83 m yr^{-1} . However, during the 20th century both a period (1913-

272 1940) with more rapid warming (0.8°C) and faster tree migration rate (1.23 m yr⁻¹) as well as a period (1940-1980) with
273 a cooling trend (-0.3°C) and stationary treeline occurred (Fig. 5). Between 1913-2000, the lower boundary of the
274 treeline shifted upwards 2 meters, while treeline upper boundaries shifted upwards 123 m. These shifts corresponded to
275 rates of 0.03 and 1.54 m yr⁻¹, respectively. Similar rates were also found in the transects established to test the heteroge-
276 neity of treeline migration (Fig. S1.2; Table S1.1; supplementary materials) where the average migration rate was 0.87
277 (0.54 - 1.25) m yr⁻¹.

278 During the 1913-2000 period, annual air temperature at the simulated treeline warmed from -2.0°C to -0.8°C. Warming
279 occurred throughout the year but was strongest in winter and spring where temperatures increased by 3.0°C and 1.4°C,
280 respectively. In contrast, both summer and autumn temperatures warmed by only 0.6°C. The resulting winter, spring,
281 summer, and autumn air temperatures at the treeline in 1990-2000 were -8.7°C, 3.3°C, 8.8°C, and -0.1°C, respectively.
282 The increases in air temperatures were also reflected in soil temperature increases of a similar magnitude, by 2.1°C
283 from -0.8°C to 1.3°C. Winter soil temperature increased with 3.7°C from -5.6°C in 1913 to -1.9°C in 2000. The warmer
284 soil temperatures resulted in a 4.8% increase in annual net nitrogen mineralisation rate in the treeline soils over the
285 same period. In absolute numbers, nitrogen mineralisation increased from 1.29 gN m⁻² to 1.36 gN m⁻². Combined with
286 an increased nitrogen deposition load from 0.06 gN m⁻² in 1913 to 0.20 gN m⁻² in 2000 and an increased nitrogen fixa-
287 tion from 0.13 gN m⁻² to 0.18 gN m⁻², plant available nitrogen increased by 15.9%. Simulated permafrost with an active
288 layer thickness of <1.5 m was present at elevations down to 560 m a.s.l. in a few gridcells, but was always well above
289 the treeline. More shallow permafrost (active layer thickness <1 m) was only present in gridcells at elevations of 940 m
290 a.s.l. and above.

291 **3.2 Projected vegetation shifts**

292 During the 100 year projection period (2001-2100) treelines advanced between 45 (HadGEM2-AO-RCP2.6) and 195
293 (GFDL-ESM2M-RCP8.5) elevational meters in the different scenarios, corresponding to rates of 0.45 and 1.95 eleva-
294 tional meters yr⁻¹. Total LAI increased in the entire ecotone in both RCP2.6 and RCP8.5 compared to the historic (1990-
295 2000) values (Fig. 3b-c). The increase was more pronounced in RCP8.5, which also saw a large increase in low ever-
296 green shrubs (LSE) at the end of the century (2090-2100). While the forest was still dominated by IBS, evergreen trees
297 (BNE and BINE) increased and together comprised approximately 15% of total LAI. The fraction of evergreen trees in
298 the forest correlated well with the degree of warming in each scenario. Forest GPP was mainly driven by tree PFTs and
299 increased by 50% (12% - 99%) for RCP2.6 and 177% (98% - 270%) for RCP8.5. Above the treeline, low shrubs (LSS
300 and LSE) contributed most to annual GPP increases, which increased by 33% (-12% - 67%) and 239% (105% - 370%)
301 in RCP2.6 and RCP8.5, respectively. Forest NPP, wherein IBS was always dominant, increased from 200 gC m⁻² yr⁻¹ in
302 year 2000 to 300 (220 - 375) gC m⁻² yr⁻¹ and 490 (380 - 610) gC m⁻² yr⁻¹ for RCP 2.6 and RCP 8.5, respectively, over
303 the projection period. NPP for the same period for IBS at the treeline increased slightly from 60 gC m⁻² yr⁻¹ to 80 (74 -
304 90) gC m⁻² yr⁻¹ and 104 (80 - 116) gC m⁻² yr⁻¹ for RCP2.6 and RCP8.5. Above the treeline NPP remained low (<25 gC
305 m⁻² yr⁻¹) for IBS in all scenarios and always had a lower NPP than the most productive shrub PFT (LSE). NPP for this
306 shrub was 49 (24 - 64) gC m⁻² yr⁻¹ and 130 (81 - 180) gC m⁻² yr⁻¹. The productivity increase translated into a biomass C
307 increase of the same magnitude in both the forest and above the treeline.

308 The average summer air temperature at the treeline between the last decade in the historic and projection periods in-
309 creased by 0.3°C and 6.7°C for the coldest (GFDL-ESM2M-RCP2.6) and warmest (MIROC-ESM2M-RCP8.5) GCM
310 scenario, respectively. The advance of the 6°C JJA soil temperature isoline was more rapid than the treeline advance
311 (Fig. 4). In the two warmest scenarios (MIROC-ESM2M-RCP8.5 and HadGEM2-AO-RCP8.5) summer soil tempera-
312 tures exceeded 6°C in the whole study domain. Treeline elevations in these scenarios only reached 745 and 660 m a.s.l.,
313 respectively. Treelines advanced almost twice as fast in RCP8.5 compared to RCP2.6, 1.55 (1.10 - 1.96) m yr⁻¹ and 0.84
314 (0.44 - 1.16) m yr⁻¹, respectively.

315 **3.3 Model experiments**

316 A slight treeline advance at the end of the projection period (2090-2100) of approximately 11 elevational meters was
317 seen in the control simulation where all drivers were held constant. This revealed a lag from the historical period, likely
318 resulting from smaller trees that had established in the historic period that matured during the projection period.

319 **3.3.1 Climate change**

320 Treeline advance occurred in all climate change scenarios although the rate was not uniform throughout the projection
321 period (Fig. 5). When driven by climate change alone, migration rates were faster than the projection simulations where
322 nitrogen deposition and CO₂ were also changed (section 3.2). Treeline advance in climate change only scenarios ranged
323 between 60 elevational meters (HadGEM2-AO-RCP2.6) to 245 elevational meters (MIROC-ESM-CHEM-RCP8.5)
324 over the 100 year projection period.

325 Tree productivity was strongly enhanced by air temperature over the whole study domain (Fig. 6a). Other climate fac-
326 tors such as precipitation and net shortwave radiation also correlated with productivity, however, these correlations
327 were weaker (Fig. S1.5; S1.6; supplementary materials). Annual precipitation increased in all climate change scenarios
328 (Table 2). In the lower parts of the valley, the increased precipitation did not result in any increased soil moisture during
329 summer as losses through evapotranspiration driven by temperature exceeded the additional input. Spring and autumn
330 soil moisture increased in the forest, mainly because of earlier snowmelt and thawing ground in spring and a relatively
331 weaker evapotranspiration in autumn. Above the treeline, soil moisture increased as the lower temperatures and LAI did
332 not drive evapotranspiration as strongly as in the lower parts of the valley and the increased rain thus outweighed the
333 slightly increased evapotranspiration.

334 Increased tree productivity in the forest resulted in an increased LAI of 18-90%, which in absolute terms was equivalent
335 to an increased LAI of 0.3-1.5 m² m⁻². BNE appeared in the forest and dominated in a few gridcells. In most places
336 BNE constituted approximately 5% of total LAI. Tall shrub (HSE and HSS) productivity and LAI increased in the for-
337 est, however, the increase was negatively correlated with temperature, i.e., increase was highest in the coldest climate
338 change scenarios. Above the treeline, tall shrubs showed the opposite pattern, increasing by 8-50% to finally constitute
339 10-36% of total LAI.

340 Higher soil moisture content in spring and autumn favoured trees in the whole ecotone, while forest understory suffered
341 from earlier onset of the growing season with subsequent flushing of the leaf and light shading from taller competitors.

342 Although soil moisture in summers decreased in the forest, LAI and biomass carbon of summergreen shrubs were posi-
343 tively correlated with soil moisture. A higher soil moisture during summers in the wetter GCM scenarios promoted
344 summergreen shrubs over evergreen shrubs in the whole ecotone. As an example, vegetation composition on the tundra
345 above the treeline differed between the two GCMs GFDL-ESM2M and MIROC-ESM-CHEM under RCP8.5, where the
346 warmer GCM showed a 52% biomass C increase in the tall evergreen shrub, HSE. The intermediately warmed scenario
347 (GFDL-ESM2M-RCP8.5) showed a more mixed increase of biomass carbon in HSE (20%) and HSS (24%). While
348 annual temperature differed with 3.9°C between the two scenarios, average annual precipitation only differed by 6.2
349 mm, yielding a much (26%) lower JJA soil moisture in the warmest scenario (MIROC-ESM-CHEM-RCP8.5) compared
350 to the colder (GFDL-ESM2M-RCP8.5). A relatively higher soil moisture and subsequently lower water stress allow for
351 taller plants to establish.

352 Radiation correlated positively with the growth of tree PFTs, with spring and autumn radiation found to be especially
353 important for height and biomass increase (Fig. S1.7; supplementary materials). Increased radiation provided a competi-
354 tive advantage for taller trees and shrubs to shade out lower shrubs and grasses in the forest. Shrubs above the treeline
355 were also favoured by increased light.

356 Net nitrogen mineralisation, i.e., the difference between microbial nitrogen mineralisation and immobilisation, at the
357 treeline showed great variation between different climate change scenarios, ranging from a 4% decrease in one scenario
358 (GFDL-ESM2M-RCP8.5) to a 79% increase in the strongest warming scenario (MIROC-ESM-CHEM- RCP8.5). In
359 absolute terms, the latter increase corresponds to an increase from 1.35 gN m⁻² yr⁻¹ at the end of our historic period
360 (1990-2000) to 2,43 g N m⁻² yr⁻¹ at the end of the century (2090-2100). This is comparable to the nitrogen load in the
361 7.5x increased nitrogen deposition scenario. Interestingly, despite very different plant available nitrogen and warming,
362 the two scenarios displayed a similar resulting (2090-2100) treeline elevation (Fig. 5a).

363 Permafrost with an active layer thickness of <1.5m disappeared completely from our study domain in all scenarios
364 except the coldest (GFDL-ESM2M-RCP2.6) where it occurred in a few gridcells at elevations of approximately 600 m
365 a.s.l. However, the shallow permafrost (<1m) had disappeared also in this scenario.

366 3.3.2 CO₂

367 Productivity increase in most PFTs correlated well with a [CO₂] increase (Fig. 6b). Total GPP averaged over the forest
368 increased between 2-10% depending on the [CO₂] scenario, with the largest increase in RCP8.5 and smallest in RCP2.6.
369 The CO₂ fertilisation effect was not uniform within the landscape, but stronger towards the forest edge with increases
370 from 2% to 18% from the weakest to the strongest [CO₂] scenario. IBS NPP increased uniformly over the forest with
371 2.5-8.4% but decreased above the treeline. Thus, the productivity of the two dominant PFTs (IBS in the forest and LSE
372 above the treeline) was reinforced in their respective domains. The increased productivity translated into a 1-5% in-
373 crease in tree LAI in the forest while low shrub LAI increased with 24-77%. Likewise, increase in leaf area of low
374 shrubs was largest on the tundra under elevated [CO₂], which saw a 15-40% LAI increase in the low and high [CO₂]
375 scenario respectively. Above the treeline, the productivity of grasses and low shrubs responded strongly to the CO₂
376 fertilisation with a 350% increase in GPP for grasses and 150% increase for low shrubs. The additional litter fall pro-

377 duced by the increased leaf mass did not lead to any increase in N mineralisation. However, immobilisation of nitrogen
378 through increased uptake by microbes increased with 2-6% between the lowest and highest [CO₂] scenarios, yielding a
379 net reduction of plant available nitrogen. Furthermore, the productivity increase did not drive any range shift of the
380 forest, i.e., the treeline remained stationary in all [CO₂] scenarios (Fig. 5b).

381 **3.3.3 Nitrogen deposition**

382 Productivity of woody PFTs was in general positively correlated with nitrogen concentration in the different nitrogen
383 deposition scenarios. In contrast, productivity of grasses was negatively correlated (Fig. 6c) as they suffered in the light
384 competition with the trees. Annual GPP of trees (especially IBS) was positively correlated throughout the whole eco-
385 tone, however, the increase in GPP was larger towards the forest boundaries than in the lower parts the forest when
386 nitrogen was added. Nitrogen stressed plants in the model allocate more carbon to their roots at the expense of foliar
387 cover when they suffer a productivity reduction. In the two scenarios with decreasing nitrogen deposition (RCP2.6;
388 RCP8.5) there was an overall reduction in LAI in both the tundra and the forest of a magnitude 6-10%. The largest
389 reduction was seen in tree PFTs, which have the largest biomass and consequently could be assumed to have the highest
390 nitrogen demand, followed by tall shrubs. Low shrubs and grasses did however increase their LAI in the forest when
391 nitrogen input decreased resulting from a decreased light competition from trees. Above the treeline, LAI of low shrubs
392 and grasses PFTs also decreased with less nitrogen input.

393 In all scenarios with increasing nitrogen deposition there was an advancement of the treeline in the order of 10-85 ele-
394 vational meters with smallest (2x nitrogen deposition) having the smallest change in treeline elevation and vice versa
395 for largest input (10x nitrogen deposition) scenario (Fig. 5c). In the scenarios where nitrogen input was constant or
396 decreasing, the treeline remained stationary.

397 **4. Discussion**

398 In our simulations, rates of treeline advance were faster under climate change-only scenarios than when all drivers were
399 changing. This revealed nitrogen as a modulating environmental variable, as nitrogen deposition was prescribed to
400 decrease in both the RCP2.6 and RCP8.5 scenarios. In contrast to previous modelling studies of treeline advance (e.g.,
401 Paulsen and Körner, 2014), we include not only temperature dependence on vegetation change, but also the full nitro-
402 gen cycle and CO₂ fertilisation effects (Smith et al., 2014). Increased nitrogen deposition induced treeline advance,
403 further illustrating the importance of nitrogen dynamics in our results. In the elevated [CO₂] scenarios, higher produc-
404 tivity in all plants was induced, but productivity enhancements alone did not lead to significant treeline advance. Fur-
405 thermore, although NPP for IBS was lower at the treeline than in the forest, it was never close to zero. Such a pattern,
406 which was seen above the treeline, would have indicated a stagnant growth, and that the productivity and carbon costs
407 of maintaining a larger biomass would have cancelled each other out. However, enhancement of productivity in combi-
408 nation with an allocation shift to the plant canopies, enabled by a greater nitrogen uptake, favoured taller plants over
409 their shorter neighbours in the competition for light within the model. Field experiments with nitrogen fertilisation have
410 shown that mountain birch at the treeline displays additional growth after nitrogen additions (Sveinbjörnsson et al.,
411 1992). Furthermore, fertilisation with nitrogen improved birch seedling survival above the treeline (Grau et al., 2012),

412 and is thus likely important for establishment and growth of new individuals to form a new treeline. As has also been
413 pointed out by others (Hofgaard et al., 2019; Van Bogaert et al., 2011), considering climate change or temperature alone
414 in projections of treeline advance could potentially result in overestimations of vegetation change. Our results clearly
415 indicate the importance of nitrogen cycling when predicting future Arctic vegetation shifts.

416 The treelines in our projection simulations advanced at similar rates to those experienced during the historic period,
417 resulting in a displacement of 45-195 elevational meters over the 100 year projection period. Some estimates based on
418 lake sediments in the Torneträsk region from the Holocene thermal maximum, when summer temperatures could have
419 been about 2.5°C warmer than present (Kullman and Kjällgren, 2006), indicate potential treeline elevations approxi-
420 mately 500m above present in the area in a warmer climate, although these elevations are likely overestimated
421 (Kullman, 2010). Macrofossil records from lakes in the area indicate that birch was present 300-400 meters above the
422 current treeline (Barnekow, 1999). Furthermore, pine might have occurred approximately 100-150 meters above its
423 present distribution (Berglund et al., 1996). IBS emerged as the dominant forest and treeline PFT in both our historic
424 and projection simulations, but with larger fractions of evergreen trees (BNE and BINE) at the end of the century
425 (2090-2100). Mountain birch, represented by IBS in our model, has historically dominated this area, even during warm-
426 er periods of the Holocene (Berglund et al., 1996), but with larger populations of pine (BINE) and spruce (BNE) than
427 present. Both pine and spruce have been found in high elevation lake pollen sediments, and can thus be assumed to have
428 grown in higher parts of the ecotone during warmer periods (Kullman, 2010). Treeline advance for the historic period in
429 our simulations is broadly consistent with observational studies from the Abisko region (Van Bogaert et al., 2011).
430 Temperature was a strong driver of tree productivity and growth in the whole ecotone. During our historic period rates
431 of treeline advance followed periods of stronger warming. However, other factors such as precipitation indirectly influ-
432 enced treeline advance through changes in vegetation composition and nitrogen mineralisation. This was illustrated by
433 the comparison of the GCMs GFDL-ESM2M and MIROC-ESM-CHEM under RCP8.5, where the more intermediately
434 warmed but wetter scenario had very similar resulting treeline elevation as the warmer scenario. While simulated
435 treeline position was too low compared to the treeline elevation reported by Callaghan et al. (2013), the correlation with
436 the globally observed 6-7°C ground temperature isohaline (Körner and Paulsen, 2004) throughout the historic period gives
437 confidence in the model results. However, during our projection period the correlation between the treeline position and
438 the 6-7°C isohaline weakened, revealing a fading or potential lag of the treeline-climate equilibrium that became stronger
439 with increased warming.

440 IBS at the treeline had a positive carbon balance (NPP) and was thus not directly limited by its productivity in our simu-
441 lations. This is consistent with observations of ample carbon storage in treeline trees globally (Hoch and Körner, 2012).
442 The modelled treeline is thus not set by productivity directly but rather by competition, as other PFTs become more
443 productive above the treeline. Whether the treeline is set by productivity constraints or by cold temperature limits on
444 wood formation and meristematic activity has been a subject of some discussion (Körner, 2015, 2003; Körner et al.,
445 2016; Fatichi et al., 2019; Pugh et al., 2016). DVMs have traditionally assumed photosynthesis to be constraining for
446 growth, and thus species distributions. On the other hand, trees close to the treeline have not shown any shortage of
447 carbon for growth (Hoch and Körner, 2012). Furthermore, enhancement of photosynthesis through added CO₂ has also
448 not always resulted in increased tree growth close to the treelines (Dawes et al., 2013), and wood formation is slow
449 around 5°C, leading to a hypothesis of reversed control of plant productivity and range distributions of trees (Körner,

450 2015). Lately, ecological interactions as a component in the control of treeline position, rather than just considering
451 hard limits to species distributions, has been a subject of more attention in modelling studies (See for ex., Scherrer et
452 al., 2020). These studies add an extra dimension to the discussion as they do not only consider plant physiology but also
453 broadly accepted ecological concepts such as realised versus fundamental niches.

454 The model overestimated biomass carbon densities in the forest but captured historic rates of biomass carbon increase.
455 The overestimation was more severe closer to the forest boundaries as the model showed a weaker negative correlation
456 between biomass carbon and elevation than observed by Hedenås et al. (2011). The mean annual biomass carbon in-
457 crease in the same dataset is, although highly variable, on average $2.5 \text{ gC m}^{-2} \text{ yr}^{-1}$ between 1997 and 2010. As simulated
458 GPP and LAI were within the range of observations in the area (Rundqvist et al., 2011; Ovhed and Holmgren, 1996;
459 Olsson et al., 2017), this indicates a coupling between photosynthesis and growth in the model that is stronger than
460 observed. Terrestrial biosphere models often overestimate biomass in high latitudes (Pugh et al., 2016; Leuzinger et al.,
461 2013) and potentially lack processes that likely limit growth close to low temperature boundaries. Examples of such
462 processes are carbon costs of nitrogen acquisition (Shi et al., 2016), including costs for mycorrhizal interactions
463 (Vowles et al., 2018), and temperature limits on growth increment (Friend et al., 2019), i.e., decoupling of growth and
464 photosynthesis. However, data on carbon allocation and its temperature dependence is scarce (Fatichi et al., 2019).
465 Additionally, the overestimation in our study can be partly attributed to lack of herbivory in the model. Outbreaks of the
466 moth *Epirrita autumnata* are known to limit productivity and reduce biomass of mountain birch in the area in certain
467 years (Olsson et al., 2017), however, this is likely not enough to explain our biomass carbon overestimation. Since
468 growth and biomass increment in the model do not include a direct temperature dependence, nor any decoupling of
469 growth and productivity, we do not regard these mechanisms as necessary to accurately predict treeline dynamics.
470 However, they might be important to accurately predict forest biomass towards their low temperature boundaries. To
471 assess the modelled heterogeneity of treeline advance, we established a number of transects close to observation points
472 in the landscape. Average treeline advance in the transects showed a somewhat faster and more homogenous migration
473 than reported (Van Bogaert et al., 2011). The model does not include historic anthropogenic disturbances, topographic
474 barriers, or insect herbivory, all of which have been documented as important for the heterogeneity of the treeline ad-
475 vance rates and placement in the landscape (Van Bogaert et al., 2011; Emanuelsson, 1987). Furthermore, our model
476 does not include any wind related processes such as wind mediated snow transport or compaction. Thus, our simula-
477 tions result in a homogenous snowpack during the winter months with no differentiation in sheltering or frost damage
478 that may result from different snow and ice properties. Sheltered locations in the landscape are known to promote sur-
479 vival of tree saplings (Sundqvist et al., 2008). For nitrogen cycling this may also mean that suggested snow-shrub feed-
480 backs (Sturm et al., 2001; Sturm, 2005) are not possible to capture with the current version of our model. While overall
481 rates of advance were captured, local variations arising from physical barriers such as steep slopes, stony patches or
482 anthropogenic disturbances were consequently not possible to capture as these processes are not implemented in the
483 model. High-resolution, local observations of vertically-resolved soil texture and soil organic matter content (see, e.g.
484 Hengl et al. (2017) for an example compiled using machine-learning) have the potential to improve the spatial variabil-
485 ity of modelled soil temperatures and nutrient cycling in our study domain. We will investigate this uncertainty in future
486 studies

487 A longer growing season favoured tree PFTs in the whole ecotone, which escaped early-season desiccation due to mild-
488 er winters and earlier spring thaw. Permafrost was only present at the highest elevations during the historic simulation
489 but had disappeared from the landscape at the end of the century for all except the coldest scenario (GFDL-ESM2M-
490 RCP2.6). The simulated permafrost was however always well above the treeline and did not have a significant impact
491 on the treeline advancement. While some aspects of ground freezing are accounted for in the model, soil vertical and
492 horizontal movement caused by frost, and amelioration of such effects in the warmer future climate are not. Such pro-
493 cesses could affect survival and competition among the plant functional types, especially in the seedling stage when
494 plants are most vulnerable to mechanical disturbance (Holtmeier and Broll, 2007). These effects could be relevant to
495 treeline dynamics at the high grid resolution of our study but are not accounted for by our model.

496 Higher summer soil moisture in the more precipitation rich climate scenarios shifted the ratio of summergreen to ever-
497 green shrubs in favour of the summergreen shrubs, in line with observations (Elmendorf et al., 2012). Conversely, drier
498 scenarios yielded an increased abundance of evergreen shrubs, similar to what has been observed in drier parts of the
499 tundra heath in the Abisko region (Scharn et al., 2021). Within RCP8.5, the warmest (MIROC-ESM-CHEM-RCP8.5)
500 and coldest (GFDL-ESM2M-RCP8.5) scenario gave rise to very similar treeline positions at the end of the projection
501 period (2090-2100). The colder scenario had both higher soil moisture and a greater abundance of summergreen shrubs.
502 Higher soil moisture promoted a larger carbon allocation to the canopy, and thus favoured the taller IBS tree PFT over
503 tall shrubs (HSS). Increased shrub abundance and nutrient cycling have been shown to have potentially non-linear ef-
504 fects on shrub growth and ecosystem carbon cycling (Buckeridge et al., 2009; Hicks et al., 2019), and some observa-
505 tions indicate that changes in the ratio of summergreen to evergreen shrubs, or an increased abundance of trees, might
506 have far-reaching consequences for soil carbon loss (Parker et al., 2018; Clemmensen et al., 2021). Thus, our results
507 indicate that any future change in soil moisture conditions could play an important role in the competitive outcome of
508 shrubs in the forest-tundra ecotone and for its carbon balance.

509 LPJ-GUESS assumes the presence of seeds in all gridcells and PFTs may establish when the 20-year (running) average
510 climate is within PFT-specific bioclimatic limits for establishment. This assumption may overlook potential constraints
511 on plant migration rates such as seed dispersal and reproduction. On larger spatial scales, it is likely that lags in range
512 shifts would arise from these additional constraints (Rees et al., 2020; Brown et al., 2018). Models that account for
513 dispersal limitations generally predict slower latitudinal tree migration than models driven solely by climate (Epstein et
514 al., 2007). However, on smaller spatial scales, the same models predict competitive interactions to be more dominant in
515 determining species migration rates (Scherrer et al., 2020). In a seed transplant study from the Swiss alps, seed viability
516 could not be shown to decline towards the range limits of eight European broadleaved tree species (Kollas et al., 2012;
517 Körner et al., 2016). Similarly, gene flow above the treeline could not be shown to be limited to near-treeline trees in
518 the Abisko region (Truong et al., 2007). Furthermore, tree saplings have been reported to be common up to 100m above
519 the present treeline (Sundqvist et al., 2008; Hofgaard et al., 2009). As environmental conditions improve, these individ-
520 uals may form the new treeline. Thus, on the scales considered in this study, we do not regard dispersal limitations as a
521 major factor in limiting range shifts of trees.

522 Above the treeline low evergreen shrubs (LSE) dominated the vegetation in both our historic and projection simula-
523 tions. The productivity of shrubs and grasses was greatly enhanced by CO₂ fertilisation in our [CO₂] model experiment,

524 and a large proportion of tundra productivity increases in our projection simulations could be attributed to rising [CO₂].
525 Physiological effects of elevated CO₂ on Arctic and alpine tundra productivity and growth are understudied. Free Air
526 CO₂ Enrichment (FACE) experiments are generally considered the best method for quantifying long-term ecosystem
527 effects of elevated CO₂ but are extremely costly and therefore limited in number and distribution. A majority of FACE
528 experiments have been implemented in temperate forests and grasslands, yielding limited evidence of relevance to bo-
529 real and tundra ecosystems (Hickler et al., 2008). One FACE experiment situated in a forest-tundra ecotone in the Swiss
530 Alps showed differing responses to elevated CO₂ among shrub species where *Vaccinium myrtillus* showed 11% in-
531 creased shoot growth while *Empetrum nigrum* was unresponsive and the response of *V. gaultherioides* depended on the
532 forest type in which it was growing (Dawes et al., 2013). Our model results indicated that shrubs are carbon limited and
533 shrub productivity and growth consequently are responsive to CO₂ fertilisation.

534 **5. Conclusions**

535 In this study we identified nitrogen cycling and availability as an important modulator of treeline advance. Internal
536 cycling of nutrients in soils is the main source of nutrients for Arctic plants (Chapin, 1983). The model performed well
537 regarding rates of shrub increase and treeline advance but overestimated biomass carbon in the forest. Treeline migra-
538 tion rates were realistically simulated although the model did not represent temperature limitations on tree growth.
539 While a decoupling between productivity and growth in the model could potentially have improved estimates of bio-
540 mass carbon, it was not needed to correctly predict treeline elevation. Instead, our results point to the importance of
541 indirect effects of rising temperatures on tree range shifts, especially with regards to nutrient cycling. Furthermore, soil
542 moisture strongly influenced vegetation composition within the model with implications for treeline advance. How
543 models represent nutrient uptake and cycling, as well as a better empirical understanding of processes that determine
544 tree and shrub growth will be key to better predictions of Arctic vegetation change and carbon and nitrogen cycling.
545 Models are a valuable aid in judging the relevance of these processes on the pan-Arctic scale.

546 **6. Author contributions**

547 AG designed the experiments with contributions from PM and SO. AG also performed necessary model code develop-
548 ments and carried out model simulations and data analysis. RGB and BS contributed greatly with comments on the
549 manuscript, scientific advice, and input throughout the study. AG prepared the manuscript with contributions from all
550 co-authors.

551 **7. Competing interests**

552 The authors declare that they have no conflict of interest.

553 **8. Acknowledgements**

554 We acknowledge the Lund University Strategic Research Areas BECC and MERGE for their financial support. Abisko
555 Scientific Research Station generously shared the data used in preparation of the future climate projections. This re-
556 search was partly funded (Paul A. Miller, Robert G. Björk) by the project BioDiv-Support through the 2017-2018 Bel-
557 mont Forum and BiodivERSA joint call for research proposals, under the BiodivScen ERA-Net COFUND programme,
558 and with the funding organisations AKA (Academy of Finland contract no 326328), ANR (ANR-18-EBI4-0007),
559 BMBF (KFZ: 01LC1810A), FORMAS (contract no:s 2018-02434, 2018-02436, 2018-02437, 2018-02438) and
560 MICINN (through APCIN: PCI2018-093149).

561 **References**

- 562 Ainsworth, E. A. and Long, S. P.: What have we learned from 15 years of free-air CO₂ enrichment (FACE)? A meta-
563 analytic review of the responses of photosynthesis, canopy properties and plant production to rising CO₂, *New Phytol*,
564 165, 351-371, 10.1111/j.1469-8137.2004.01224.x, 2005.
- 565 Barnekow, L.: Holocene tree-line dynamics and inferred climatic changes in the Abisko area, northern Sweden, based on
566 macrofossil and pollen records, *The Holocene*, 9, 253-265, 1999.
- 567 Batjes, N. H.: ISRIC-WISE global data set of derived soil properties on a 0.5 by 0.5 degree grid (version 3.0), ISRIC –
568 World Soil Information, Wageningen, 2005.
- 569 Berglund, B. E., Barnekow, L., Hammarlund, D., Sandgren, P., and Snowball, I. F.: Holocene forest dynamics and
570 climate changes in the Abisko area, northern Sweden - the Sonesson model of vegetation history reconsidered and
571 confirmed, *Ecological Bulletins*, 45, 15-30, 1996.
- 572 Bhatt, U. S., Walker, D. A., Raynolds, M. K., Comiso, J. C., Epstein, H. E., Jia, G., Gens, R., Pinzon, J. E., Tucker, C.
573 J., Tweedie, C. E., and Webber, P. J.: Circumpolar Arctic Tundra Vegetation Change Is Linked to Sea Ice Decline,
574 *Earth Interactions*, 14, 1-20, 10.1175/2010ei315.1, 2010.
- 575 Björkman, A. D., Myers-Smith, I. H., Elmendorf, S. C., Normand, S., Ruger, N., Beck, P. S. A., Blach-Overgaard, A.,
576 Blok, D., Cornelissen, J. H. C., Forbes, B. C., Georges, D., Goetz, S. J., Guay, K. C., Henry, G. H. R., HilleRisLambers,
577 J., Hollister, R. D., Karger, D. N., Kattge, J., Manning, P., Prevey, J. S., Rixen, C., Schaepman-Strub, G., Thomas, H. J.
578 D., Vellend, M., Wilmking, M., Wipf, S., Carbognani, M., Hermanutz, L., Levesque, E., Molau, U., Petraglia, A.,
579 Soudzilovskaia, N. A., Spasojevic, M. J., Tomaselli, M., Vowles, T., Alatalo, J. M., Alexander, H. D., Anadon-Rosell,
580 A., Angers-Blondin, S., Beest, M. T., Berner, L., Björk, R. G., Buchwal, A., Buras, A., Christie, K., Cooper, E. J.,
581 Dullinger, S., Elberling, B., Ekelinen, A., Frei, E. R., Grau, O., Grogan, P., Hallinger, M., Harper, K. A., Heijmans,
582 M., Hudson, J., Hulber, K., Iturrate-Garcia, M., Iversen, C. M., Jaroszynska, F., Johnstone, J. F., Jorgensen, R. H.,
583 Kaarlejarvi, E., Klady, R., Kuleza, S., Kulonen, A., Lamarque, L. J., Lantz, T., Little, C. J., Speed, J. D. M., Michelsen,
584 A., Milbau, A., Nabe-Nielsen, J., Nielsen, S. S., Ninot, J. M., Oberbauer, S. F., Olofsson, J., Onipchenko, V. G., Rumpf,

585 S. B., Semenchuk, P., Shetti, R., Collier, L. S., Street, L. E., Suding, K. N., Tape, K. D., Trant, A., Treier, U. A.,
586 Tremblay, J. P., Tremblay, M., Venn, S., Weijers, S., Zamin, T., Boulanger-Lapointe, N., Gould, W. A., Hik, D. S.,
587 Hofgaard, A., Jonsdottir, I. S., Jorgenson, J., Klein, J., Magnusson, B., Tweedie, C., Wookey, P. A., Bahn, M., Blonder,
588 B., van Bodegom, P. M., Bond-Lamberty, B., Campetella, G., Cerabolini, B. E. L., Chapin, F. S., 3rd, Cornwell, W. K.,
589 Craine, J., Dainese, M., de Vries, F. T., Diaz, S., Enquist, B. J., Green, W., Milla, R., Niinemets, U., Onoda, Y.,
590 Ordonez, J. C., Ozinga, W. A., Penuelas, J., Poorter, H., Poschlod, P., Reich, P. B., Sandel, B., Schamp, B.,
591 Sheremetev, S., and Weiher, E.: Plant functional trait change across a warming tundra biome, *Nature*, 562, 57-62,
592 10.1038/s41586-018-0563-7, 2018.

593 Brown, C. D., Dufour - Tremblay, G., Jameson, R. G., Mamet, S. D., Trant, A. J., Walker, X. J., Boudreau, S., Harper,
594 K. A., Henry, G. H. R., Hermanutz, L., Hofgaard, A., Isaeva, L., Kershaw, G. P., and Johnstone, J. F.: Reproduction as
595 a bottleneck to treeline advance across the circumarctic forest tundra ecotone, *Ecography*, 42, 137-147,
596 10.1111/ecog.03733, 2018.

597 Bruhwiler, L., Parmentier, F.-J. W., Crill, P., Leonard, M., and Palmer, P. I.: The Arctic Carbon Cycle and Its Response
598 to Changing Climate, *Current Climate Change Reports*, 7, 14-34, 10.1007/s40641-020-00169-5, 2021.

599 Buckeridge, K. M., Zufelt, E., Chu, H., and Grogan, P.: Soil nitrogen cycling rates in low arctic shrub tundra are
600 enhanced by litter feedbacks, *Plant and Soil*, 330, 407-421, 10.1007/s11104-009-0214-8, 2009.

601 Cairns, D. and Moen, J.: Herbivory Influences Tree Lines, *Journal of Ecology*, 92, 1019-1024, 2004.

602 Callaghan, T. V., Jonasson, C., Thierfelder, T., Yang, Z., Hedenas, H., Johansson, M., Molau, U., Van Bogaert, R.,
603 Michelsen, A., Olofsson, J., Gwynn-Jones, D., Bokhorst, S., Phoenix, G., Bjerke, J. W., Tommervik, H., Christensen, T.
604 R., Hanna, E., Koller, E. K., and Sloan, V. L.: Ecosystem change and stability over multiple decades in the Swedish
605 subarctic: complex processes and multiple drivers, *Philos Trans R Soc Lond B Biol Sci*, 368, 20120488,
606 10.1098/rstb.2012.0488, 2013.

607 Chapin, F. S., 3rd, Sturm, M., Serreze, M. C., McFadden, J. P., Key, J. R., Lloyd, A. H., McGuire, A. D., Rupp, T. S.,
608 Lynch, A. H., Schimel, J. P., Beringer, J., Chapman, W. L., Epstein, H. E., Euskirchen, E. S., Hinzman, L. D., Jia, G.,
609 Ping, C. L., Tape, K. D., Thompson, C. D., Walker, D. A., and Welker, J. M.: Role of land-surface changes in arctic
610 summer warming, *Science*, 310, 657-660, 10.1126/science.1117368, 2005.

611 Chapin, F. S. I.: Direct and Indirect Effects of Temperature on Arctic Plants, *Polar Biology*, 2, 47-52, 1983.

612 Clemmensen, K. E., Durling, M. B., Michelsen, A., Hallin, S., Finlay, R. D., and Lindahl, B. D.: A tipping point in
613 carbon storage when forest expands into tundra is related to mycorrhizal recycling of nitrogen, *Ecol Lett*, 24, 1193-
614 1204, 10.1111/ele.13735, 2021.

615 Cleveland, C. C., Townsend, A. R., Schimel, D. S., Fisher, H., Howarth, R. W., Hedin, L. O., Perakis, S. S., Latty, E.
616 F., Von Fischer, J. C., Elseroad, A., and Wasson, M. F.: Global patterns of terrestrial biological nitrogen (N₂) fixation
617 in natural ecosystems, *Global Biogeochemical Cycles*, 13, 623-645, 10.1029/1999gb900014, 1999.

618 Dawes, M. A., Hagedorn, F., Handa, I. T., Streit, K., Ekblad, A., Rixen, C., Körner, C., and Hättenschwiler, S.: An
619 alpine treeline in a carbon dioxide-rich world: synthesis of a nine-year free-air carbon dioxide enrichment study,
620 *Oecologia*, 171, 623-637, 10.1007/s00442-012-2576-5, 2013.

621 Dusenge, M. E., Duarte, A. G., and Way, D. A.: Plant carbon metabolism and climate change: elevated CO₂ and
622 temperature impacts on photosynthesis, photorespiration and respiration, *New Phytol*, 221, 32-49, 10.1111/nph.15283,
623 2019.

624 Elmendorf, S. C., Henry, G. H. R., Hollister, R. D., Björk, R. G., Boulanger-Lapointe, N., Cooper, E. J., Cornelissen, J.
625 H. C., Day, T. A., Dorrepaal, E., Elumeeva, T. G., Gill, M., Gould, W. A., Harte, J., Hik, D. S., Hofgaard, A., Johnson,
626 D. R., Johnstone, J. F., Jónsdóttir, I. S., Jorgenson, J. C., Klanderud, K., Klein, J. A., Koh, S., Kudo, G., Lara, M.,
627 Lévesque, E., Magnússon, B., May, J. L., Mercado-Dí'az, J. A., Michelsen, A., Molau, U., Myers-Smith, I. H.,
628 Oberbauer, S. F., Onipchenko, V. G., Rixen, C., Martin Schmidt, N., Shaver, G. R., Spasojevic, M. J., Pórhallsdóttir, P.
629 E., Tolvanen, A., Troxler, T., Tweedie, C. E., Villareal, S., Wahren, C.-H., Walker, X., Webber, P. J., Welker, J. M.,
630 and Wipf, S.: Plot-scale evidence of tundra vegetation change and links to recent summer warming, *Nature Climate*
631 *Change*, 2, 453-457, 10.1038/nclimate1465, 2012.

632 Emanuelsson, U.: Human Influence on Vegetation in the Torneträsk Area during the Last Three Centuries, *Ecological*
633 *Bulletins*, 38, 95-111, 1987.

634 Epstein, H. E., Kaplan, J. O., Lischke, H., and Yu, Q.: Simulating Future Changes in Arctic and Subarctic Vegetation,
635 *Computing in Science & Engineering*, 9, 12-23, 10.1109/mcse.2007.84, 2007.

636 Epstein, H. E., Raynolds, M. K., Walker, D. A., Bhatt, U. S., Tucker, C. J., and Pinzon, J. E.: Dynamics of aboveground
637 phytomass of the circumpolar Arctic tundra during the past three decades, *Environmental Research Letters*, 7,
638 10.1088/1748-9326/7/1/015506, 2012.

639 Fatichi, S., Pappas, C., Zscheischler, J., and Leuzinger, S.: Modelling carbon sources and sinks in terrestrial vegetation,
640 *New Phytol*, 221, 652-668, 10.1111/nph.15451, 2019.

641 Forbes, B. C., Fauria, M. M., and Zetterberg, P.: Russian Arctic warming and 'greening' are closely tracked by tundra
642 shrub willows, *Global Change Biology*, 16, 1542-1554, 10.1111/j.1365-2486.2009.02047.x, 2010.

643 Friend, A. D., Eckes-Shephard, A. H., Fonti, P., Rademacher, T. T., Rathgeber, C. B. K., Richardson, A. D., and
644 Turton, R. H.: On the need to consider wood formation processes in global vegetation models and a suggested
645 approach, *Annals of Forest Science*, 76, 10.1007/s13595-019-0819-x, 2019.

646 Grau, O., Ninot, J. M., Blanco-Moreno, J. M., van Logtestijn, R. S. P., Cornelissen, J. H. C., and Callaghan, T. V.:
647 Shrub-tree interactions and environmental changes drive treeline dynamics in the Subarctic, *Oikos*, 121, 1680-1690,
648 10.1111/j.1600-0706.2011.20032.x, 2012.

649 Hallinger, M., Manthey, M., and Wilmking, M.: Establishing a missing link: warm summers and winter snow cover
650 promote shrub expansion into alpine tundra in Scandinavia, *New Phytologist*, 186, 890-899, 10.1111/j.1469-
651 8137.2010.0322, 2010.

652 Harsch, M. A., Hulme, P. E., McGlone, M. S., and Duncan, R. P.: Are treelines advancing? A global meta-analysis of
653 treeline response to climate warming, *Ecol Lett*, 12, 1040-1049, 10.1111/j.1461-0248.2009.01355.x, 2009.

654 Hedenås, H., Olsson, H., Jonasson, C., Bergstedt, J., Dahlberg, U., and Callaghan, T. V.: Changes in Tree Growth,
655 Biomass and Vegetation Over a 13-Year Period in the Swedish Sub-Arctic, *Ambio*, 40, 672-682, 10.1007/s13280-011-
656 0173-1, 2011.

657 Hengl, T., Mendes de Jesus, J., Heuvelink, G. B., Ruiperez Gonzalez, M., Kilibarda, M., Blagotic, A., Shangguan, W.,
658 Wright, M. N., Geng, X., Bauer-Marschallinger, B., Guevara, M. A., Vargas, R., MacMillan, R. A., Batjes, N. H.,
659 Leenaars, J. G., Ribeiro, E., Wheeler, I., Mantel, S., and Kempen, B.: SoilGrids250m: Global gridded soil information
660 based on machine learning, *PLoS One*, 12, e0169748, 10.1371/journal.pone.0169748, 2017.

661 Hickler, T., Smith, B., Prentice, I. C., MjÖFors, K., Miller, P., Arneth, A., and Sykes, M. T.: CO2 fertilization in
662 temperate FACE experiments not representative of boreal and tropical forests, *Global Change Biology*, 14, 1531-1542,
663 10.1111/j.1365-2486.2008.01598.x, 2008.

664 Hicks, L. C., Rousk, K., Rinnan, R., and Rousk, J.: Soil Microbial Responses to 28 Years of Nutrient Fertilization in a
665 Subarctic Heath, *Ecosystems*, 23, 1107-1119, 10.1007/s10021-019-00458-7, 2019.

666 Hoch, G. and Körner, C.: Global patterns of mobile carbon stores in trees at the high-elevation tree line, *Global Ecology*
667 *and Biogeography*, 21, 861-871, 10.1111/j.1466-8238.2011.00731.x, 2012.

668 Hofgaard, A., Dalen, L., and Hytteborn, H.: Tree recruitment above the treeline and potential for climate-driven treeline
669 change, *Journal of Vegetation Science*, 20, 1133-1144, 2009.

670 Hofgaard, A., Harper, K. A., and Golubeva, E.: The role of the circumarctic forest-tundra ecotone for Arctic
671 biodiversity, *Biodiversity*, 13, 174-181, 10.1080/14888386.2012.700560, 2012.

672 Hofgaard, A., Ols, C., Drobyshev, I., Kirchhefer, A. J., Sandberg, S., and Söderström, L.: Non-stationary Response of
673 Tree Growth to Climate Trends Along the Arctic Margin, *Ecosystems*, 22, 434-451, 10.1007/s10021-018-0279-4, 2019.

- 674 Holtmeier, F. K. and Broll, G. E.: Treeline advance - driving processes and adverse factors, *Landscape Online*, 1, 1-33,
675 10.3097/lo.200701, 2007.
- 676 Josefsson, M.: *The Geoecology of Subalpine Heaths in the Abisko Valley, Northern Sweden. A study of periglacial*
677 *conditions.*, Department of Physical Geography, Uppsala University, Sweden, 180 pp., 1990.
- 678 Karlsson, P. S. and Weih, M.: Relationships between Nitrogen Economy and Performance in the Mountain Birch *Betula*
679 *pubescens ssp. tortuosa*, *Ecological Bulletins*, 71-78, 1996.
- 680 Kollas, C., Vitasse, Y., Randin, C. F., Hoch, G., and Korner, C.: Unrestricted quality of seeds in European broad-leaved
681 tree species growing at the cold boundary of their distribution, *Ann Bot*, 109, 473-480, 10.1093/aob/mcr299, 2012.
- 682 Kullman, L.: A richer, greener and smaller alpine world: review and projection of warming-induced plant cover change
683 in the Swedish Scandes, *Ambio*, 39, 159-169, 10.1007/s13280-010-0021-8, 2010.
- 684 Kullman, L. and KjÄLLgren, L.: Holocene pine tree-line evolution in the Swedish Scandes: Recent tree-line rise and
685 climate change in a long-term perspective, *Boreas*, 35, 159-168, 10.1111/j.1502-3885.2006.tb01119.x, 2006.
- 686 Körner, C.: Carbon limitation in trees, *Journal of Ecology*, 91, 4-17, 2003.
- 687 Körner, C.: Paradigm shift in plant growth control, *Curr Opin Plant Biol*, 25, 107-114, 10.1016/j.pbi.2015.05.003, 2015.
- 688 Körner, C. and Paulsen, J.: A World-Wide Study of High Altitude Treeline Temperatures, *Journal of Biogeography*, 31,
689 713-732, 2004.
- 690 Körner, C., Basler, D., Hoch, G., Kollas, C., Lenz, A., Randin, C. F., Vitasse, Y., and Zimmermann, N. E.: Where, why
691 and how? Explaining the low-temperature range limits of temperate tree species, *Journal of Ecology*, 104, 1079-1088,
692 10.1111/1365-2745.12574, 2016.
- 693 Lamarque, J. F., Dentener, F., McConnell, J., Ro, C. U., Shaw, M., Vet, R., Bergmann, D., Cameron-Smith, P.,
694 Dalsoren, S., Doherty, R., Faluvegi, G., Ghan, S. J., Josse, B., Lee, Y. H., MacKenzie, I. A., Plummer, D., Shindell, D.
695 T., Skeie, R. B., Stevenson, D. S., Strode, S., Zeng, G., Curran, M., Dahl-Jensen, D., Das, S., Fritzsche, D., and Nolan,
696 M.: Multi-model mean nitrogen and sulfur deposition from the Atmospheric Chemistry and Climate Model
697 Intercomparison Project (ACCMIP): evaluation of historical and projected future changes, *Atmospheric Chemistry and*
698 *Physics*, 13, 7997-8018, 10.5194/acp-13-7997-2013, 2013.
- 699 Leuzinger, S., Manusch, C., Bugmann, H., and Wolf, A.: A sink-limited growth model improves biomass estimation
700 along boreal and alpine tree lines, *Global Ecology and Biogeography*, 22, 924-932, 10.1111/geb.12047, 2013.

701 McGuire, A. D., Anderson, L. G., Christensen, T. R., Dallimore, S., Guo, L., Hayes, D. J., Heimann, M., Lorenson, T.
702 D., Macdonald, R. W., and Roulet, N.: Sensitivity of the carbon cycle in the Arctic to climate change, *Ecological*
703 *Monographs*, 79, 523-555, 10.1890/08-2025.1, 2009.

704 McGuire, A. D., Christensen, T. R., Hayes, D., Heroult, A., Euskirchen, E., Kimball, J. S., Koven, C., Lafleur, P.,
705 Miller, P. A., Oechel, W., Peylin, P., Williams, M., and Yi, Y.: An assessment of the carbon balance of Arctic tundra:
706 comparisons among observations, process models, and atmospheric inversions, *Biogeosciences*, 9, 3185-3204,
707 10.5194/bg-9-3185-2012, 2012.

708 Miller, P. A. and Smith, B.: Modelling tundra vegetation response to recent arctic warming, *Ambio*, 41 Suppl 3, 281-
709 291, 10.1007/s13280-012-0306-1, 2012.

710 Myers-Smith, I. H., Hik, D. S., and Aerts, R.: Climate warming as a driver of tundra shrubline advance, *Journal of*
711 *Ecology*, 106, 547-560, 10.1111/1365-2745.12817, 2018.

712 Myers-Smith, I. H., Forbes, B. C., Wilmking, M., Hallinger, M., Lantz, T., Blok, D., Tape, K. D., Macias-Fauria, M.,
713 Sass-Klaassen, U., Lévesque, E., Boudreau, S., Ropars, P., Hermanutz, L., Trant, A., Collier, L. S., Weijers, S.,
714 Rozema, J., Rayback, S. A., Schmidt, N. M., Schaepman-Strub, G., Wipf, S., Rixen, C., Ménard, C. B., Venn, S.,
715 Goetz, S., Andreu-Hayles, L., Elmendorf, S., Ravolainen, V., Welker, J., Grogan, P., Epstein, H. E., and Hik, D. S.:
716 Shrub expansion in tundra ecosystems: dynamics, impacts and research priorities, *Environmental Research Letters*, 6,
717 10.1088/1748-9326/6/4/045509, 2011.

718 Myers-Smith, I. H., Elmendorf, S. C., Beck, P. S. A., Wilmking, M., Hallinger, M., Blok, D., Tape, K. D., Rayback, S.
719 A., Macias-Fauria, M., Forbes, B. C., Speed, J. D. M., Boulanger-Lapointe, N., Rixen, C., Lévesque, E., Schmidt, N.
720 M., Baittinger, C., Trant, A. J., Hermanutz, L., Collier, L. S., Dawes, M. A., Lantz, T. C., Weijers, S., Jørgensen, R. H.,
721 Buchwal, A., Buras, A., Naito, A. T., Ravolainen, V., Schaepman-Strub, G., Wheeler, J. A., Wipf, S., Guay, K. C., Hik,
722 D. S., and Vellend, M.: Climate sensitivity of shrub growth across the tundra biome, *Nature Climate Change*, 5, 887-
723 891, 10.1038/nclimate2697, 2015.

724 Olsson, P.-O., Heliasz, M., Jin, H., and Eklundh, L.: Mapping the reduction in gross primary productivity in subarctic
725 birch forests due to insect outbreaks, *Biogeosciences*, 14, 1703-1719, 10.5194/bg-14-1703-2017, 2017.

726 Ovhed, M. and Holmgren, B.: Modelling and measuring evapotranspiration in a mountain birch forest, *Ecological*
727 *Bulletins*, 45, 31-44, 1996.

728 Parker, T. C., Sanderman, J., Holden, R. D., Blume-Werry, G., Sjogersten, S., Large, D., Castro-Diaz, M., Street, L. E.,
729 Subke, J. A., and Wookey, P. A.: Exploring drivers of litter decomposition in a greening Arctic: results from a
730 transplant experiment across a treeline, *Ecology*, 99, 2284-2294, 10.1002/ecy.2442, 2018.

731 Paulsen, J. and Körner, C.: A climate-based model to predict potential treeline position around the globe, *Alpine*
732 *Botany*, 124, 1-12, 10.1007/s00035-014-0124-0, 2014.

733 Piao, S., Sitch, S., Ciais, P., Friedlingstein, P., Peylin, P., Wang, X., Ahlstrom, A., Anav, A., Canadell, J. G., Cong, N.,
734 Huntingford, C., Jung, M., Levis, S., Levy, P. E., Li, J., Lin, X., Lomas, M. R., Lu, M., Luo, Y., Ma, Y., Myneni, R. B.,
735 Poulter, B., Sun, Z., Wang, T., Viovy, N., Zaehle, S., and Zeng, N.: Evaluation of terrestrial carbon cycle models for
736 their response to climate variability and to CO₂ trends, *Glob Chang Biol*, 19, 2117-2132, 10.1111/gcb.12187, 2013.

737 Pugh, T. A. M., Muller, C., Arneth, A., Haverd, V., and Smith, B.: Key knowledge and data gaps in modelling the
738 influence of CO₂ concentration on the terrestrial carbon sink, *J Plant Physiol*, 203, 3-15, 10.1016/j.jplph.2016.05.001,
739 2016.

740 Rees, W. G., Hofgaard, A., Boudreau, S., Cairns, D. M., Harper, K., Mamet, S., Mathisen, I., Swirad, Z., and
741 Tutubalina, O.: Is subarctic forest advance able to keep pace with climate change?, *Glob Chang Biol*, 26, 3965-3977,
742 10.1111/gcb.15113, 2020.

743 Rundqvist, S., Hedenås, H., Sandström, A., Emanuelsson, U., Eriksson, H., Jonasson, C., and Callaghan, T. V.: Tree
744 and Shrub Expansion Over the Past 34 Years at the Tree-Line Near Abisko, Sweden, *Ambio*, 40, 683-692,
745 10.1007/s13280-011-0174-0, 2011.

746 Scharn, R., Brachmann, C. G., Patchett, A., Reese, H., Bjorkman, A., Alatalo, J., Björk, R. G., Jägerbrand, A. K.,
747 Molau, U., and Björkman, M. P.: Vegetation responses to 26 years of warming at Latnjajaure Field Station, northern
748 Sweden, *Arctic Science*, 10.1139/as-2020-0042, 2021.

749 Scherrer, D., Vitasse, Y., Guisan, A., Wohlgemuth, T., Lischke, H., and Gomez Aparicio, L.: Competition and
750 demography rather than dispersal limitation slow down upward shifts of trees' upper elevation limits in the Alps,
751 *Journal of Ecology*, 108, 2416-2430, 10.1111/1365-2745.13451, 2020.

752 Serreze, M. C. and Barry, R. G.: Processes and impacts of Arctic amplification: A research synthesis, *Global and*
753 *Planetary Change*, 77, 85-96, 10.1016/j.gloplacha.2011.03.004, 2011.

754 Shi, M., Fisher, J. B., Brzostek, E. R., and Phillips, R. P.: Carbon cost of plant nitrogen acquisition: global carbon cycle
755 impact from an improved plant nitrogen cycle in the Community Land Model, *Glob Chang Biol*, 22, 1299-1314,
756 10.1111/gcb.13131, 2016.

757 Smith, B., Prentice, I. C., and Sykes, M. T.: Representation of vegetation dynamics in the modelling of terrestrial
758 ecosystems: comparing two contrasting approaches within European climate space, *Global Ecology and Biogeography*,
759 10, 621-637, 10.1046/j.1466-822X.2001.t01-1-00256.x, 2001.

760 Smith, B., Wårlind, D., Arneth, A., Hickler, T., Leadley, P., Siltberg, J., and Zaehle, S.: Implications of incorporating N
761 cycling and N limitations on primary production in an individual-based dynamic vegetation model, *Biogeosciences*, 11,
762 2027-2054, 10.5194/bg-11-2027-2014, 2014.

763 Sturm, M.: Changing snow and shrub conditions affect albedo with global implications, *Journal of Geophysical*
764 *Research*, 110, 10.1029/2005jg000013, 2005.

765 Sturm, M., Holmgren, J., McFadden, J. P., Liston, G. E., Chapin, F. S., and Racine, C. H.: Snow–Shrub Interactions in
766 Arctic Tundra: A Hypothesis with Climatic Implications, *Journal of Climate*, 14, 336-344, 10.1175/1520-
767 0442(2001)014<0336:Ssiat>2.0.Co;2, 2001.

768 Sullivan, P., Ellison, S., McNown, R., Brownlee, A., and Sveinbjörnsson, B.: Evidence of soil nutrient availability as
769 the proximate constraint on growth of treeline trees in northwest Alaska, *Ecology*, 96, 716-727, 2015.

770 Sundqvist, M. K., Björk, R. G., and Molau, U.: Establishment of boreal forest species in alpine dwarf-shrub heath in
771 subarctic Sweden, *Plant Ecology & Diversity*, 1, 67-75, 10.1080/17550870802273395, 2008.

772 Sveinbjörnsson, B., Nordell, O., and Kauhanen, H.: Nutrient relations of mountain birch growth at and below the
773 elevational tree-line in Swedish Lapland, *Functional Ecology*, 6, 213-220, 1992.

774 Taylor, K. E., Stouffer, R. J., and Meehl, G. A.: An Overview of CMIP5 and the Experiment Design, *Bulletin of the*
775 *American Meteorological Society*, 93, 485-498, 10.1175/bams-d-11-00094.1, 2012.

776 Truong, C., Palme, A. E., and Felber, F.: Recent invasion of the mountain birch *Betula pubescens* ssp. *tortuosa* above
777 the treeline due to climate change: genetic and ecological study in northern Sweden, *J Evol Biol*, 20, 369-380,
778 10.1111/j.1420-9101.2006.01190.x, 2007.

779 Van Bogaert, R., Haneca, K., Hoogesteger, J., Jonasson, C., De Dapper, M., and Callaghan, T. V.: A century of tree line
780 changes in sub-Arctic Sweden shows local and regional variability and only a minor influence of 20th century climate
781 warming, *Journal of Biogeography*, 38, 907-921, 10.1111/j.1365-2699.2010.02453.x, 2011.

782 Virkkala, A. M., Aalto, J., Rogers, B. M., Tagesson, T., Treat, C. C., Natali, S. M., Watts, J. D., Potter, S., Lehtonen,
783 A., Mauritz, M., Schuur, E. A. G., Kochendorfer, J., Zona, D., Oechel, W., Kobayashi, H., Humphreys, E., Goeckede,
784 M., Iwata, H., Lafleur, P. M., Euskirchen, E. S., Bokhorst, S., Marushchak, M., Martikainen, P. J., Elberling, B., Voigt,
785 C., Biasi, C., Sonnentag, O., Parmentier, F. W., Ueyama, M., Celis, G., St Loius, V. L., Emmerton, C. A., Peichl, M.,
786 Chi, J., Jarveoja, J., Nilsson, M. B., Oberbauer, S. F., Torn, M. S., Park, S. J., Dolman, H., Mammarella, I., Chae, N.,
787 Poyatos, R., Lopez-Blanco, E., Rojle Christensen, T., Jung Kwon, M., Sachs, T., Holl, D., and Luoto, M.: Statistical
788 upscaling of ecosystem CO₂ fluxes across the terrestrial tundra and boreal domain: regional patterns and uncertainties,
789 *Glob Chang Biol*, 10.1111/gcb.15659, 2021.

790 Vowles, T., Lindwall, F., Ekblad, A., Bahram, M., Furneaux, B. R., Ryberg, M., and Bjork, R. G.: Complex effects of
791 mammalian grazing on extramatrical mycelial biomass in the Scandes forest-tundra ecotone, *Ecol Evol*, 8, 1019-1030,
792 10.1002/ece3.3657, 2018.

793 Wania, R., Ross, I., and Prentice, I. C.: Integrating peatlands and permafrost into a dynamic global vegetation model: 1.
794 Evaluation and sensitivity of physical land surface processes, *Global Biogeochemical Cycles*, 23, n/a-n/a,
795 10.1029/2008gb003412, 2009.

796 Wei, Y., Liu, S., Huntzinger, D. N., Michalak, A. M., Viovy, N., Post, W. M., Schwalm, C. R., Schaefer, K., Jacobson,
797 A. R., Lu, C., Tian, H., Ricciuto, D. M., Cook, R. B., Mao, J., and Shi, X.: The North American Carbon Program Multi-
798 scale Synthesis and Terrestrial Model Intercomparison Project – Part 2: Environmental driver data, *Geoscientific Model*
799 *Development*, 7, 2875-2893, 10.5194/gmd-7-2875-2014, 2014.

800 Weih, M. and Karlsson, S.: The nitrogen economy of mountain birch seedlings: implications for winter survival,
801 *Journal of Ecology*, 87, 211-219, 1999.

802 Wolf, A., Callaghan, T. V., and Larson, K.: Future changes in vegetation and ecosystem function of the Barents Region,
803 *Climatic Change*, 87, 51-73, 10.1007/s10584-007-9342-4, 2008.

804 Yang, Z., Hanna, E., and Callaghan, T. V.: Modelling surface - air - temperature variation over complex terrain around
805 abisko, swedish lapland: uncertainties of measurements and models at different scales, *Geografiska Annaler: Series A,*
806 *Physical Geography*, 93, 89-112, 10.1111/j.1468-0459.2011.00005.x, 2011.

807 Yang, Z., Hanna, E., Callaghan, T. V., and Jonasson, C.: How can meteorological observations and microclimate
808 simulations improve understanding of 1913-2010 climate change around Abisko, Swedish Lapland?, *Meteorological*
809 *Applications*, 19, 454-463, 10.1002/met.276, 2012.

810 Zhang, W., Jansson, C., Miller, P. A., Smith, B., and Samuelsson, P.: Biogeophysical feedbacks enhance the Arctic
811 terrestrial carbon sink in regional Earth system dynamics, *Biogeosciences*, 11, 5503-5519, 10.5194/bg-11-5503-2014,
812 2014.

813 Zhang, W., Miller, P. A., Jansson, C., Samuelsson, P., Mao, J., and Smith, B.: Self-Amplifying Feedbacks Accelerate
814 Greening and Warming of the Arctic, *Geophysical Research Letters*, 45, 7102-7111, 10.1029/2018gl077830, 2018.

815 Zhang, W., Miller, P. A., Smith, B., Wania, R., Koenigk, T., and Döscher, R.: Tundra shrubification and tree-line
816 advance amplify arctic climate warming: results from an individual-based dynamic vegetation model, *Environmental*
817 *Research Letters*, 8, 10.1088/1748-9326/8/3/034023, 2013.

818

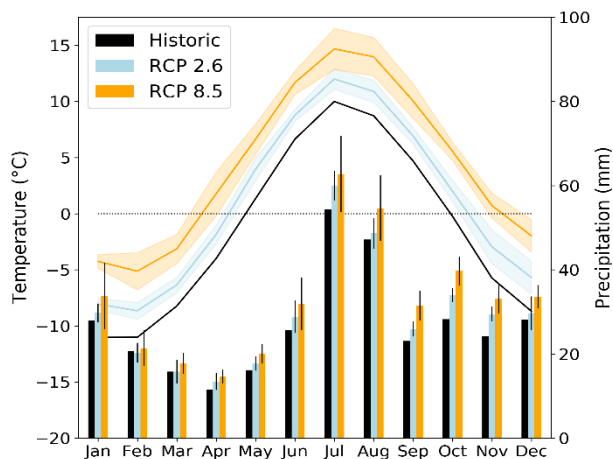


Figure 1. Historic (1971-2000) and projected (2071-2100) temperature (left) and precipitation (right) variability in Abisko. The shaded areas (temperature) and black bars (precipitation) mark ± 1 standard deviation uncertainty in the three CMIP5 multi-model mean for RCP2.6 and RCP8.5 respectively.

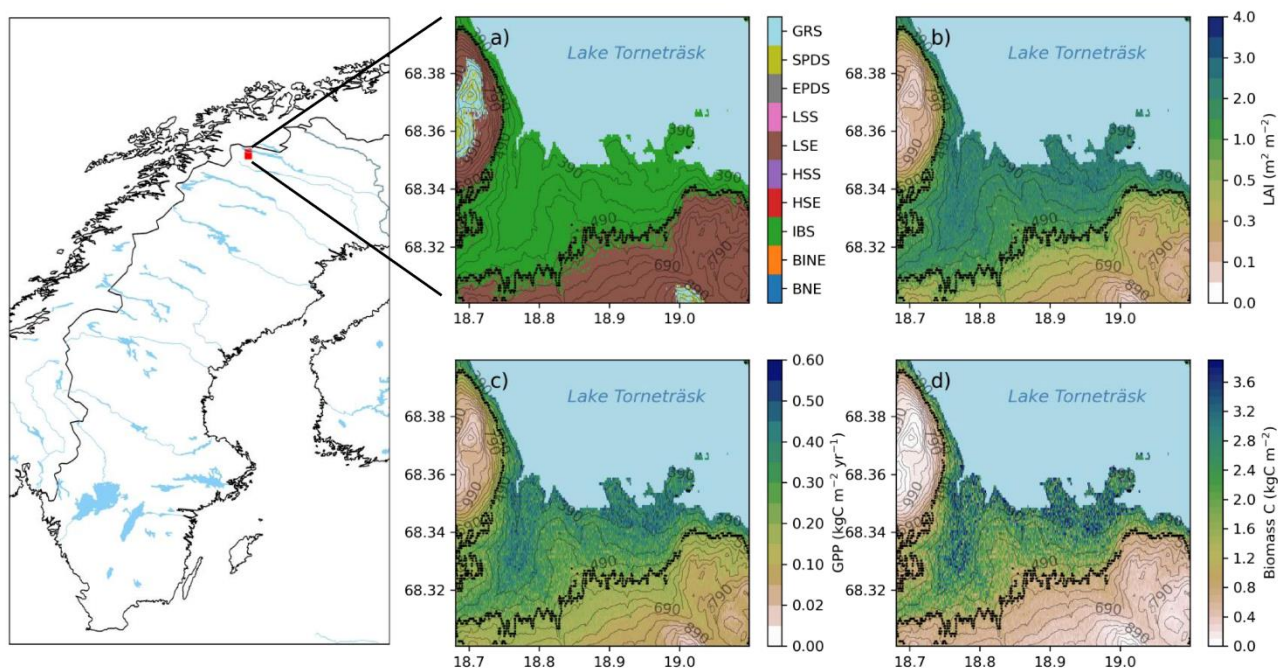


Figure 2. Map of Sweden and Scandinavia with a red square marking the study area. Panels on the right show the study area in more detail and the modelled forest-tundra ecotone for the historic period (1990-2000). a) Dominant PFT (BNE – Boreal needle leaved evergreen tree; BINE – Boreal shade-intolerant needle leaved tree; IBS – Boreal shade-intolerant broadleaved tree; HSE – Tall evergreen shrub; HSS – Tall summergreen shrub; LSE – Low evergreen shrub; LSS – Low summergreen shrub; EPDS – Evergreen prostrate dwarf shrub; SPDS – Summergreen prostrate dwarf shrub; GRS - grasses) in the ecotone and total ecosystem b) LAI ($\text{m}^2 \text{m}^{-2}$) c) productivity (GPP; $\text{kgC m}^{-2} \text{yr}^{-1}$) and d) plant biomass carbon density (kgC m^{-2}). The black line in panels a-d shows the modelled treeline position. Numbers on the contour lines mark elevation in meters above sea level. Data source for map: Natural Earth

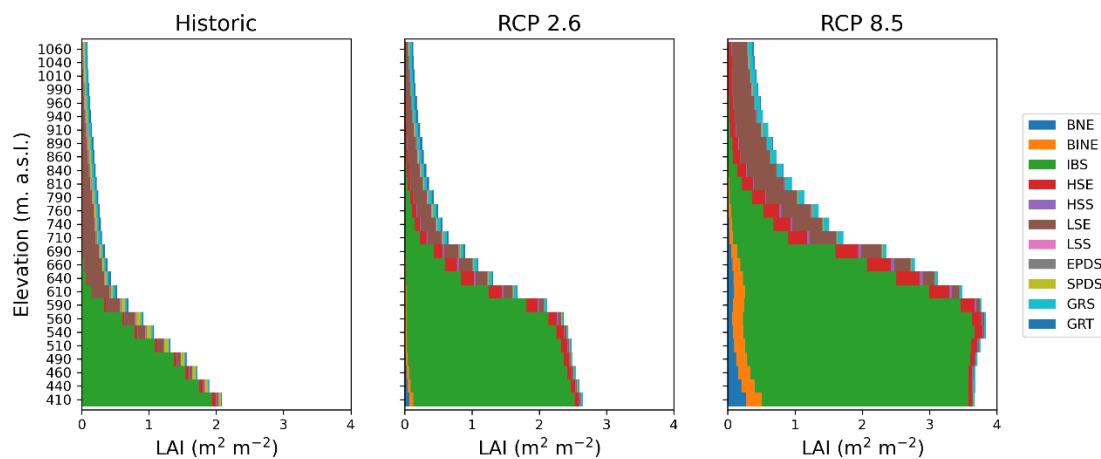


Figure 3. Leaf area index (LAI) in the forest-tundra ecotone for a) historic (1990-2000) and at the end of the century (2090-2100) for b) RCP2.6 and c) RCP8.5 respectively. Each bar represents an approximate 50 elevational meter band in the ecotone.

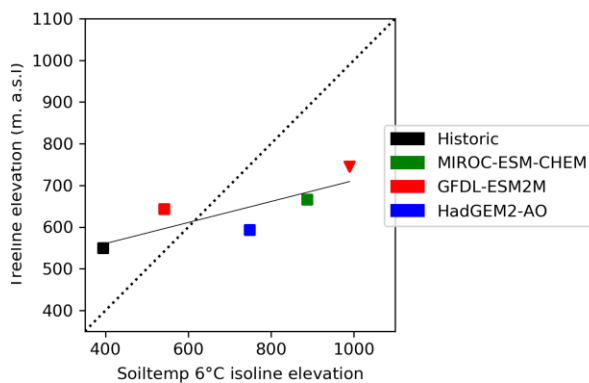


Figure 4. JJA 6°C soil temperature isoline correlation with average treeline elevation. Square markers represent RCP2.6 while triangles represent RCP8.5. In the two warmest scenarios (HadGEM2-AO-RCP8.5 and MIROC-ESM-CHEM-RCP8.5), the 6°C soil temperatures exceeded 6°C in the whole landscape. The dotted line represents the 1:1 relationship between treeline and isoline placement while the full line displays the treeline-soil temperature regression.

Table 1. Model evaluation and benchmarking results.

| Parameter | Unit | Domain | Time Interval | Model value | Estimated value | Reference |
|---|-------------------------------------|---------------|---------------|-------------|-----------------|--------------------------|
| GPP (Average) | gC m ⁻² yr ⁻¹ | Birch forest | 2007-2014 | 410 ± 64 | 440 ± 54 | Olsson et al., 2017 |
| Carbon density | tC ha ⁻¹ | Birch forest | 2010 | 21.8 ± 10 | 4.39 ± 3.46 | Hedenäs et al., 2011 |
| Carbon density change | % | Birch forest | 1997-2010 | 25 | 19 | |
| LAI | m ² m ⁻² | Forest canopy | 1988-1989 | 1.65 ± 0.66 | ~2.0 | Ovhed & Holmgren, 1996 |
| | | Understory | | 0.17 ± 0.12 | ~0.5 | |
| Densification | % | Shrub tundra | 1976-2010 | +87 ± 15 | +50-80 | Rundqvist et al., 2011 |
| Treeline elevation (min) | m. a.s.l. | Treeline | 2010 | 444 | ~600 | Callaghan et al., 2013 |
| Treeline elevation (mean) | | | | 564 | - | |
| Treeline elevation (max) | | | | 723 | ~800 | |
| Treeline elevation change (mean) | Elevational meters | Treeline | 1912-2009 | 80 | 24 | van Boogart et al., 2011 |
| Treeline elevation change (max) | | | | 123 | 145 | |
| Treeline migration rate (mean) | m yr ⁻¹ | Treeline | 1912-2009 | +0.85 | +0.6 | van Boogart et al., 2011 |
| Treeline migration rate (max) | | | | +1.18 | +1.1 | |

Table 2. Seasonal temperature and precipitation for historic and scenario simulations.

| | Season | 1971-2000 | | | 2071-2100 | | | |
|---------------------------|----------------------|-------------------|------------|--------|------------|--------|----------------|--------|
| | | Yang et al., 2011 | GFDL-ESM2M | | HadGEM2-AO | | MIROC-ESM-CHEM | |
| | | Historic | RCP2.6 | RCP8.5 | RCP2.6 | RCP8.5 | RCP2.6 | RCP8.5 |
| Temperature (°C) | Winter (DJF) | -9.8 | -8.2 | -5.4 | -8.1 | -4.4 | -7.4 | -3.1 |
| | Spring (MAM) | -2.1 | -1.3 | 1.0 | 0.4 | 4.11 | 0.7 | 4.8 |
| | Summer (JJA) | 9.9 | 10.9 | 13.2 | 11.9 | 14.4 | 13.1 | 13.4 |
| | Autumn (SON) | 0.1 | 1.1 | 4.2 | 2.3 | 9.1 | 3.2 | 7.2 |
| | Annual (mean) | -0.5 | 0.6 | 3.3 | 1.6 | 5.0 | 2.4 | 6.6 |
| Precipitation (MM) | Winter (DJF) | 75 | 80 | 85 | 75 | 80 | 70 | 95 |
| | Spring (MAM) | 45 | 40 | 45 | 40 | 45 | 50 | 55 |
| | Summer (JJA) | 125 | 130 | 130 | 130 | 150 | 135 | 145 |
| | Autumn (SON) | 75 | 90 | 95 | 85 | 95 | 95 | 110 |
| | Annual (sum) | 325 | 340 | 355 | 335 | 370 | 350 | 405 |

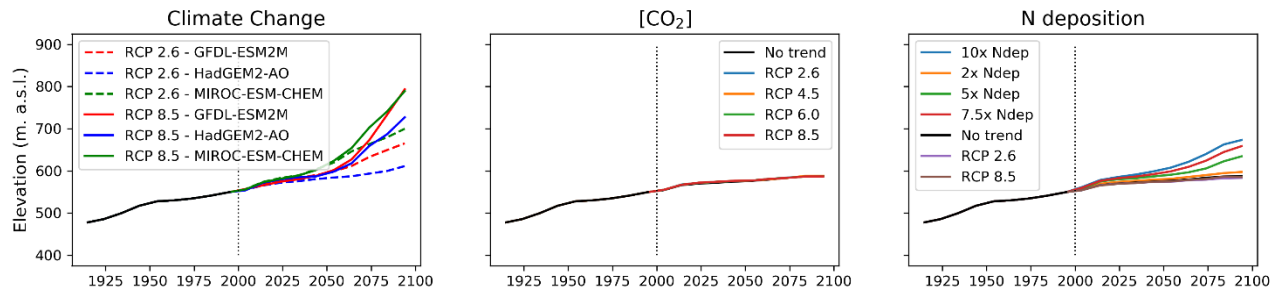


Figure 5. Shifts in average treeline elevation over the simulation period for the three experiments a) climate change b) CO₂ fertilisation and c) nitrogen deposition. Start of projection simulations are marked with a vertical dotted line in all panels. No-trend scenario in panel b-c represent a scenario where climate, CO₂ and nitrogen deposition are kept constant (without trend) relative to year 2000. Black line before year 2000 represents our historic simulation.

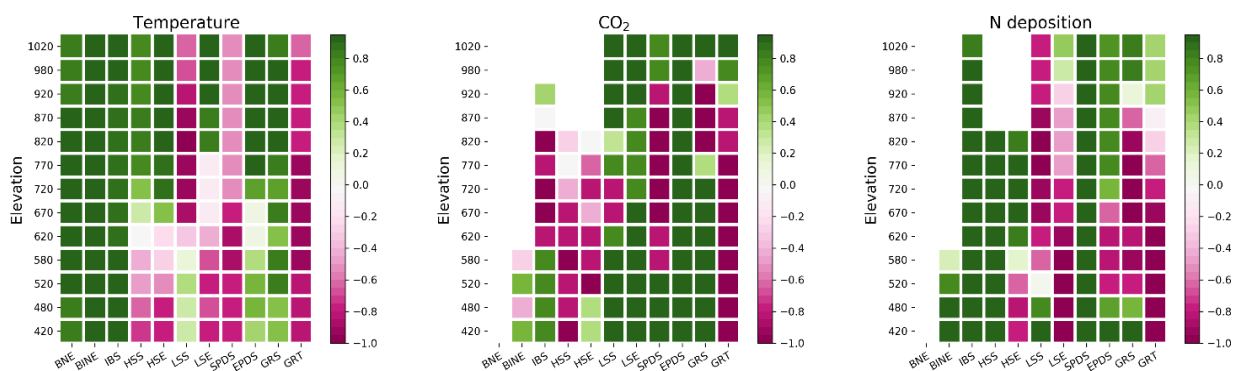


Figure 6. Correlation (Spearman rank) between annual GPP for each PFT and a) average end of century (2090-2100) temperature anomalies in the climate change experiment, b) CO₂ scenario and c) nitrogen deposition scenario. Each box represent a 50 elevational meter band in the ecotone for a given PFT.